Prog. Biophys. molec. Biol., Vol. 42, pp. 95–133, 1983.
Printed in Great Britain.

0079-6107/83 $0.00+.50

STRUCTURAL PROPERTIES OF PROTEIN β-SHEETS

F. R. SALEMME

Genex Corporation, 16020 Industrial Drive, Gaithersburg, Maryland 20877, U.S.A.

CONTENTS

I. INTRODUCTION

X-ray crystallographic studies of proteins have revealed a rich variety of structural architectures. Despite this diversity, many proteins share common features of structural organization. The extent to which proteins can be described as being structurally similar depends upon their incorporation of regular secondary structures. The observation that many proteins are predominantly composed of α-helices, antiparallel β-sheet, or a combination of α-helices and parallel β-sheet, has provided a basis for the structural classification of proteins (Levitt and Chothia, 1976; Richardson, 1981). Such classification schemes have been an important first step in understanding protein structural organization. More importantly, these studies make evident that many structural motifs recur among proteins otherwise bearing little similarity in amino acid sequence or function. The recurrence of similar structural motifs among evolutionarily unrelated proteins presumably reflects underlying physical factors which depend only in a general way on protein sequence, but nevertheless are effective determinants of protein structural organization.

The present work examines the structural properties of β-sheets in proteins. Crystallographically observed β-sheets in globular proteins exhibit an extraordinary diversity of structural forms. In contrast to the classical flat β-sheet arrangements first described by Pauling and Corey (1951), globular protein β-sheets conform to a variety of twisted and curved surfaces. A basic objective of this review is to describe the operative forces and constraints which produce different twisted β-sheet geometries. The factors involved are most readily understood by considering the properties of a classical flat structure (Fig. 1). A β-sheet is basically an aligned, planar array of conformationally regular polypeptide chains which are interconnected by hydrogen bonds. The flat sheet can be viewed as a regular, two-dimensional lattice stabilized by covalent bonds along the direction of the polypeptide chains, and by hydrogen-bonds (i.e. dipole interactions) between or across the chains. The minimum energy configuration of the lattice will generally reflect the simultaneous

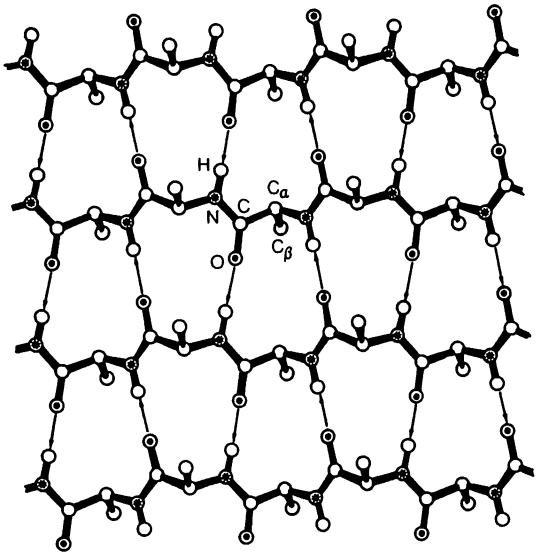

FIG. 1. Plan view of an extended, flat parallel β-sheet. The structure can be viewed as an extended lattice stabilized by covalent interactions along the polypeptide chain directions, and by dipolar or hydrogen-bonded interactions across the chains.

optimization of both the conformational energies of the individual polypeptide chains and the hydrogen-bonded interactions between them. The occurrence of a finite flat sheet would then represent a situation where the most stable conformation of the polypeptide chains produced an 180° rotational, or two-fold helical relationship between successive peptide planes. The resulting periodic and planar arrangement of the peptide groups allows formation of a flat sheet whose hydrogen-bonds are everywhere optimal and equivalent.

Observed β-sheets in globular proteins fundamentally differ from the classical flat arrangement because the polypeptide chains are composed of L-amino acids. Because the repeating subunits of the chains are chiral, they tend to assume minimum energy conformations whose effect is to twist the polypeptide chains away from the two-fold helical conformation which produces flat sheets. This in turn results in the introduction of energetically unfavorable distortions into the interchain hydrogen-bonds. The final configuration of the sheet consequently represents an energetic compromise between optimizing the conformation energy of the polypeptide chains and preserving the interchain hydrogen-bonds (Weatherford and Salemme, 1979). The final geometry of the sheet therefore depends upon the specific features of interchain hydrogen-bonding which constrain the possible ways in which the polypeptide chains can twist. The great variety of sheet geometries observed in globular proteins reflect alternative ways of reaching this compromise. As will be shown, there are two different types of constraint which manifest themselves in the generation of β-sheets with different twisted geometries. The first of these depends upon whether the polypeptide chains are arranged parallel (with the same amino to carboxy terminus sense) or antiparallel. Owing to fundamental differences in parallel vs antiparallel sheet symmetry properties, the effects of chain twisting can produce quite different structural geometries under the correspondingly different constraints imposed by the hydrogen-bonds. A second more general factor responsible for different sheet geometries emerges from the sheet's lattice properties. In general, deforming the flat sheet (Fig. 1) by twisting the chains will have the effect of propagating ever larger dislocations in the hydrogen-bonds towards the lattice periphery. Consequently, very large β-sheets are typically nearly flat (Salemme and Weatherford, 1981a,b). On the other hand, smaller sheets can accumulate the dislocations that result from chain twisting at their boundaries where periodic hydrogen bonding constraints are absent. The final geometry of the sheet will therefore additionally depend on sheet size and shape (i.e. the number, length, and hydrogen-bonding arrangement of the polypeptide chains) which effectively determine the boundary constraints on sheet twisting (Salemme, 1981).

Although a major objective of this review is to illustrate the origins of observed β-sheet geometries, it will emerge that β-sheets possess a variety of cooperative properties which reflect their underlying lattice properties. The same regular interaction patterns which provide constraints determining the final configuration of the extended structure, also define low-energy pathways for cooperative excursions of the structure from its minimum energy state. This behaviour has implications that are of considerable interest with regard to a number of physicochemical properties of proteins. Consequently, following an initial description of the factors responsible for the observed geometrical properties of β-sheets, the cooperative properties of these structures will be discussed in relation to protein dynamics, stabilization, and folding pathways for β-sheets.

II. GEOMETRICAL AND SYMMETRY PROPERTIES OF β-SHEETS

The objective of what follows is to describe the basic geometrical features of β-sheets, beginning with a description of the symmetry properties of the regular flat structures. Subsequently (Section III), it will be described how the geometrical requirements of interchain hydrogen-bonding effect constraints on sheet twisting, and more specifically, how the different symmetries of parallel and antiparallel sheets can result in quite different twisted geometries.

The classical flat β-sheet structures were first described by Pauling and Corey (1951). The structures are composed of extended polypeptide chains whose successive residues form a two-fold helix. In extended chains, this corresponds to a 180° rotation of successive planar peptide linkages about the central chain axis. The C_β substituents alternately project above and below the mean plane of the peptide linkages, and so define a second plane that is rotated $\sim 90°$ from the mean plane of the peptide groups. Two or more such chains can be brought together so that hydrogen-bonds are formed between peptide groups of adjacent chains to produce a flat β-sheet. This results in a structure whose peptide groups are contiguously connected to form an approximately planar array of hydrogen bonds, and whose surfaces are occupied by residue C_β substituents which project approximately normal to the mean sheet plane (Fig. 1).

There are two different sheet arrangements which can occur, depending on the relative amino (N) to carboxyl (C) sense of adjacent hydrogen-bonded chains. Parallel β-sheets are formed when all chains have the same N to C direction, and antiparallel sheets formed when adjacent chains are oriented in opposite N to C direction. Figure 2 illustrates some short sections of flat parallel and antiparallel β-sheet. Although both structures are composed of extended two-fold helical polypeptide chains, formation of the classical β-sheets, having linear N-H-O-C′ interchain hydrogen bonds, results in the two structures having different polypeptide chain conformations. The parallel and antiparallel structures correspond to two specific sets of ϕ, ψ backbone conformations which are consistent with slightly different geometrical requirements for interchain hydrogen-bonding. The polypeptide conformation which optimizes hydrogen-bonds between parallel strands occurs at $\phi = -116°$, $\psi = 112°$, while that for antiparallel strands occurs at $\phi = -147°$, $\psi = 145°$ (Fig. 3). These alternate conformations also result in differences in the dipeptide repeat period for the two structures (~ 6.50 Å, parallel: vs ~ 6.95 Å, antiparallel), which cause the parallel structure to have a more pronounced pleat when viewed from the edge.

Assembly of the chains into sheets results in the emergence of new symmetry elements relating residues of adjacent chains. In the case of the flat parallel sheet, adjacent chains form an interconnected set of identical hydrogen-bonded rings which are roughly trapezoidal in plan, and which incorporate residues whose C_β substituents alternately project above and below the mean plane of the sheet. The successive residue pairs comprising the hydrogen-bonded rings are therefore related by an additional 2-fold screw axis which is centrally located between the chains in the plane of the sheet (Fig. 2).

The antiparallel sheet is substantially different. In contrast to the parallel sheet, the double-strand antiparallel structure is organized as an interconnected set of "small" and "large" hydrogen-bonded rings, so that each pair of rings translationally repeats along the chain axis direction. As an additional consequence of the opposite N to C arrangement of the chains,

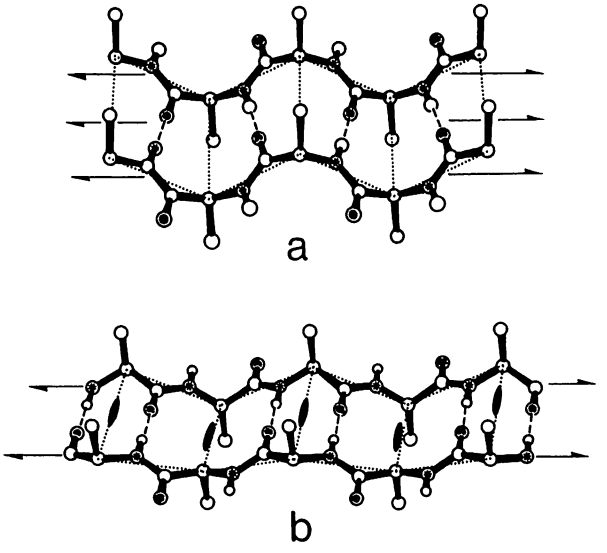

FIG. 2. β-sheets can occur in two forms that differ according to whether the chains are arranged with the same N to C sense (parallel, (a)), or opposite N to C sense (antiparallel, (b)). Half-barbed arrows indicate the orientations of two-fold screw symmetry axes, relating successive chain residues in both structures, and successive hydrogen-bonded rings in the parallel sheet. Eclipses in (b) show positions of two-fold rotation axes relating hydrogen-bonded residues in the antiparallel sheet.

dyad symmetry axes emerge which relate residues on opposite sides (i.e. adjacent chains) of each small and large hydrogen-bonded ring. These dyad symmetry axes lie normal to the mean sheet plane and are centrally located in each of the hydrogen-bonded rings (Fig. 2). Since the symmetry properties of β-sheets essentially reflect the periodic nature of interchain hydrogen-bonding, it will be seen in what follows that symmetry based approaches are most useful in investigating the twisted states of these structures as they appear in globular proteins.

III. THE GEOMETRY OF TWISTED β-SHEETS IN PROTEINS

With the advent of protein crystallographic studies, it became evident that β-sheets in globular proteins differed from the classical flat arrangements described by Pauling and Corey. Specifically, the sheets of globular proteins are nearly invariably observed to twist in a "right-handed" direction when viewed along the polypeptide chain axes (Chothia, 1973). This overall twist of the sheet reflects the introduction of twist into its substituent chains. While the chains of the classical flat sheet are two-fold helices, chains of twisted sheets have greater than two residues per helical turn (Fig. 3). The invariant right-handed twist results from the assumption of local left-handed helical character of the individual polypeptide chains. The slight left-handed chain twist produces right-twisted sheets because the interactions between adjacent chains recur between alternating residues (Fig. 4). Consequently, the cumulative effect of small successive left-handed displacements between residues i and i+1, and i+1 and i+2, is to relate peptide groups of residues i and i+2 by a right-handed helix. The tendency for extended polypeptide chains to assume left-handed helical conformations results from their incorporation of L-amino acids (described in more detail below). Therefore, the chiral properties of the sheet as a whole fundamentally reflect the chiral asymmetry of its individual amino acid subunits.

Owing to the twist of the polypeptide chains in globular protein β-sheets, they typically conform to extended surfaces of complex curvature. The variety of observed spatial geometries can nevertheless be understood from a common standpoint. Specifically, the observed geometries reflect the compensatory interaction of two factors. The first of these is the tendency of the polypeptide chain to twist, in order to minimize its conformational energy. As this property depends on local intrachain interactions, it is a common property of virtually all β-sheets, however else they may differ. The second factor involves the geometrical

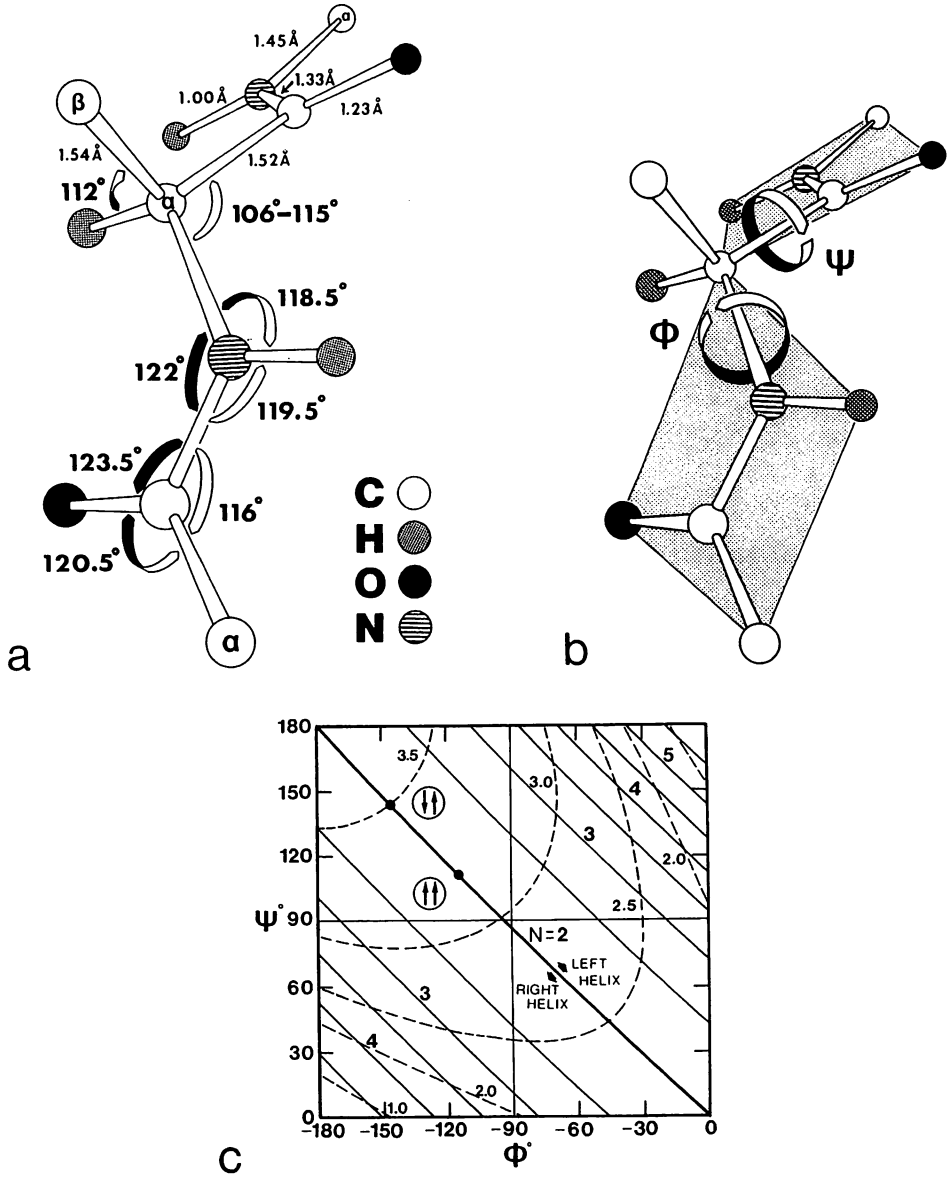

FIG. 3. Polypeptide conformation. Many features of the polypeptide chain structure, such as bond lengths, angles, and peptide bond planarity are relatively fixed (a). Alternative polypeptide structures differ in conformation, which correspond to different torsional rotations about single bonds connecting each amino acid C_α carbon to the adjacent peptide planes (b). Part (c) shows how various geometrical parameters of structures composed of conformationally identical residues vary over the range of $\phi = -180$ to 0°, and $\psi = 0$ to 180°. A given point on the plot defines a helical structure characterized by the number of residues per turn (solid lines) and the rise along the helix axis per residue (dashed lines). The classical flat β-sheets are composed of two-fold helical chains lying on the $n = 2$ line (indicated by dots and adjacent symbols). Observed sheets have slightly left-twisted chains, whose conformations lie to the right of the $n = 2$ line on the plot.

limitations on chain twist which result from the requirement for preservation of the interchain hydrogen bonds. Then nature of the constraints imposed by hydrogen-bonding differs depending both on the number and arrangement of strands in the sheet, and whether they are arranged parallel or antiparallel.

1. *Parallel Sheets*

Parallel β-sheets in proteins are almost invariably observed to occur as multiple-strand arrangements (Richardson, 1981). Typically, the sheets are situated on the protein interior

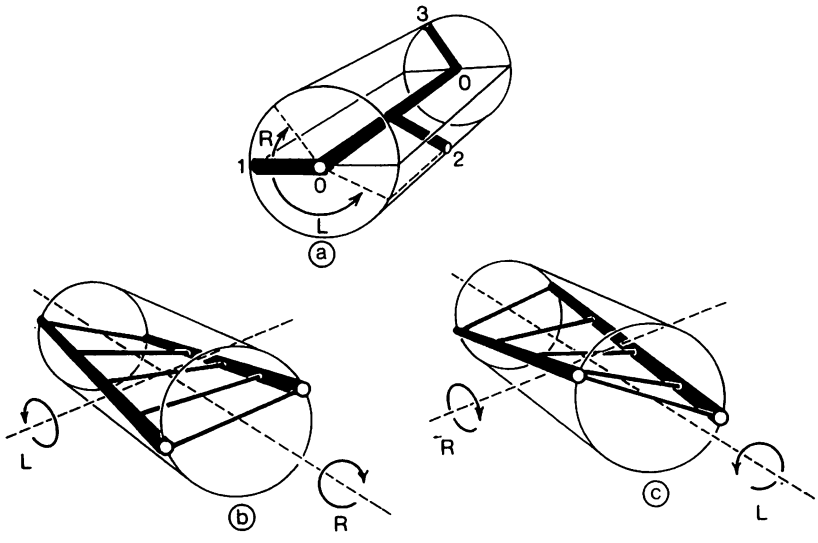

FIG. 4. Definition of twist sense in β-sheets. Chains forming twisted β-sheets have conformations lying to the right of the $n=2$ line on the ϕ, ψ plot (Fig. 3), and so are left-handed helices (a). However, interactions between sheet chains occur for alternating residues which define a right-hand helix. Extended sheets then appear to have a net right-hand twist when viewed along the chain axis direction (b). Conversely, a left-twisted sheet (c) would be composed of locally right-hand helices.

where the parallel sheet strands are interconnected by α-helices which pack on the sheet surface(s). Two different characteristic parallel sheet geometries are observed (Fig. 5). In the first arrangement the sheet as a whole conforms to a saddle-shaped surface that generally has α-helices packed on both sides. Such sheets typically have rectangular hydrogen-bond plans where there are a similar number of residues in each polypeptide chain and the hydrogen-bonds extend in register across the sheet strands. Two geometrical features of twisted rectangular plan sheets are noteworthy. First, the individual strands of these sheets are essentially straight polypeptide chains, suggesting that they approximate twisted polypeptide helices whose substituent amino acid residues have identical conformational (ϕ, ψ)

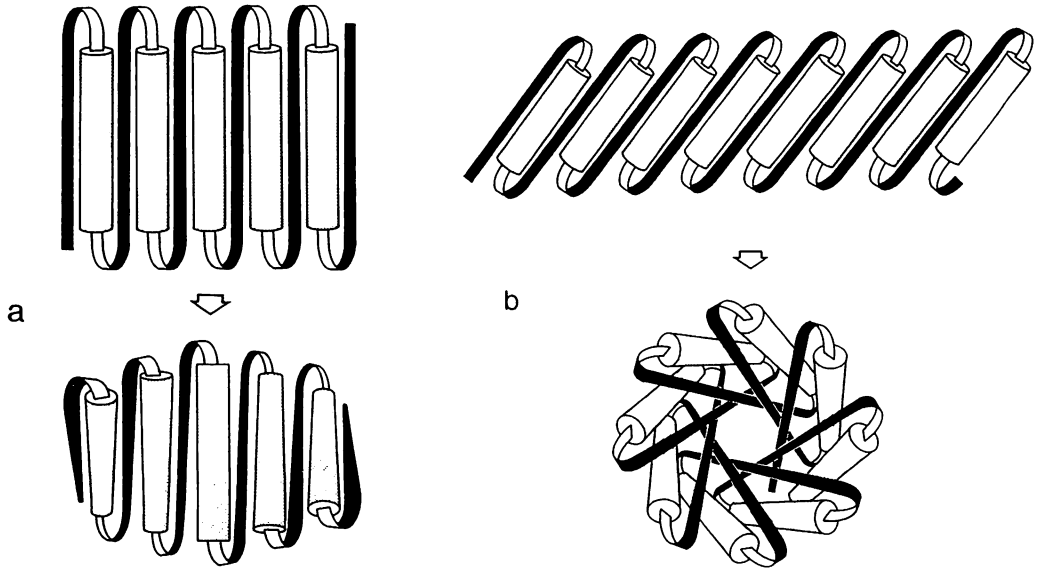

FIG. 5. Twisted parallel β-sheet geometries. Part (a) shows a rectangular-plan parallel sheet arrangement with adjacent chains interconnected by α-helices (shown as cylinders). Such arrangements form twisted saddle-shaped surfaces where the helices pack on one (or both) sides of the sheet. Part (b) shows an arrangement where both the sheet strands and helices are staggered. This arrangement forms a barrel when the β-sheet twists.

values. Second, the observed rates of twist between chains is remarkably constant throughout a given sheet (Fig. 6). This suggests that the interchain interactions, and therefore the individual chain conformations, are approximately equivalent throughout the sheet. As shown in Fig. 7, such an arrangement of straight helical chains naturally produces a saddle shaped surface (an hyperbolic paraboloid, Gellert *et al.*, 1977) as a consequence of the twisting of the individual polypeptide chains. The uniformity of interchain twist is correspondingly a consequence of the geometry of the interchain bonding; each strand incorporates planar peptide groups that interact with adjacent chains which must be similarly helical in order to optimize the uniformity of the hydrogen-bonds (Fig. 8). Nevertheless, since the chains of the sheet are essentially straight, the ends of any two adjacent chains will tend to diverge as the twist angle between them increases. In other words, twisting the sheet has the effect of stretching the hydrogen-bonds between the ends of the sheet strands. As a result, the final geometry of the observed structure reflects a compromise between the tendency of the individual chains to twist and the constraints imposed by the requirements for preservation of the interchain hydrogen-bonds. Clearly, the longer the strands within the sheet, the greater

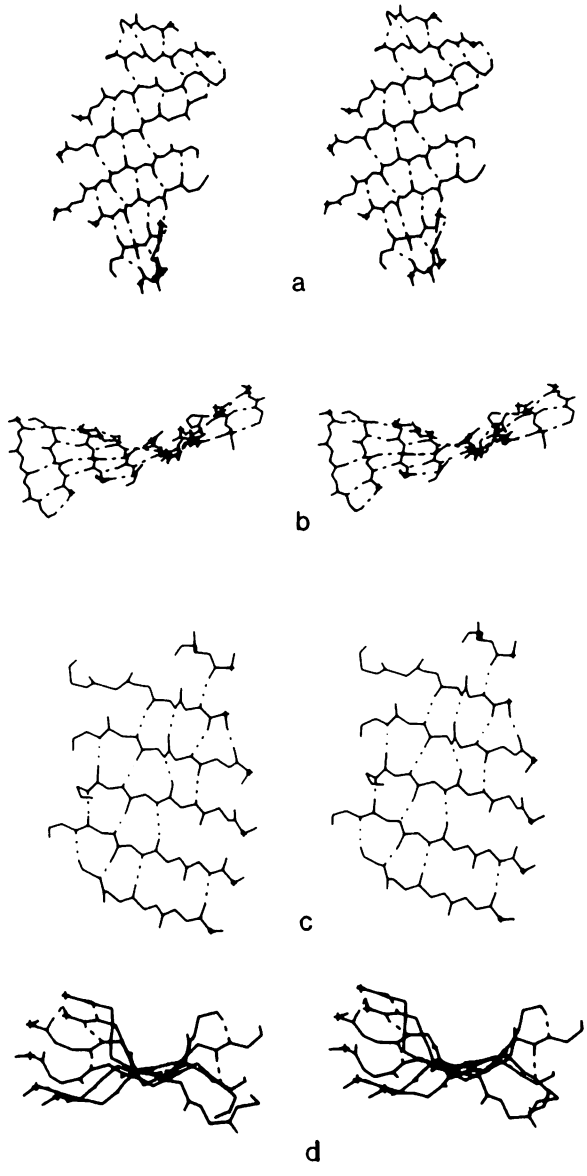

FIG. 6. Views of twisted parallel and mixed β-sheets forming saddle-shaped structural backbones in lactate dehydrogenase ((a) and (b)) and carboxypeptidase A ((c) and (d)) (Feldmann, 1976).

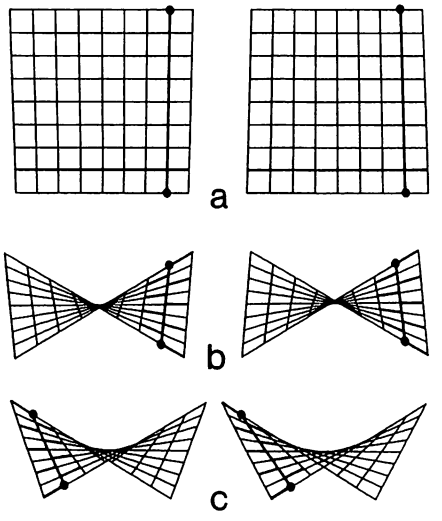

FIG. 7. Rectangular twisted sheets form surfaces which are hyperbolic paraboloids. The name derives from the fact that vertical cross-sections of maximum curvature are upward- or downward-curved parabolas, while horizontal sections are paired branches of hyperbolas. These are ruled arrays that can be generated from intersecting sets of straight lines, to produce a surface that is locally curved in opposite directions, i.e. anticlastically curved. The formation of such surfaces by twisted β-sheets reflects the twisting tendencies of the polypeptide chains, which behave as a set of helical springs (e.g. unbroken line with dotted endpoints). However, the interchain hydrogen-bonded interactions tend to resist the introduction of twist into the sheet; the extended across-the-sheet interaction effectively corresponding to a set of helical springs that are orthogonal to the polypeptide chains and which resist torsional twist. The equilibration of these opposing forces results in the attainment of an isotropically stressed surface.

the rate of divergence between the strand ends as the sheet twists. Consequently, it is both expected and observed (other factors being equal) that larger sheets will generally twist to lesser extents than sheets with fewer numbers of interchain hydrogen-bonds. Computer modelling studies, based upon the optimization of interchain hydrogen-bonded interactions between helically twisted polypeptide chains, suggest that there exist relatively well-defined chain conformations appropriate to parallel sheets with different twists (Fig. 9). As shown in Fig. 10, sheets assembled from such chains are remarkably regular and preserve good hydrogen-bonding geometry for interchain twists comparable to those observed in proteins for sheets of similar overall dimensions. In fact, it has been shown that such regular structures assembled from chains with appropriate twist typically yield atom for atom RMS fits of <1 Å vs observed structural coordinates (Salemme and Weatherford, 1981a,b). Thus, despite the multitude of additional factors which introduce local conformational perturbations (Section V), observed structures are seen to be surprisingly regular.

A second recurrent arrangement seen in a number of proteins incorporating parallel sheets is a barrel structure. Here the β-sheet forms an internal cylindrical framework where

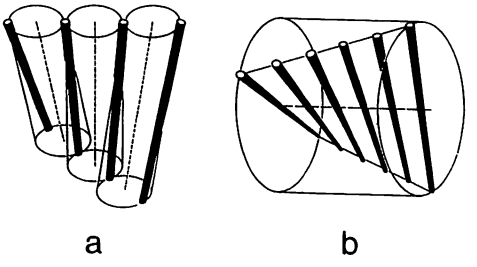

FIG. 8. A twisted β-sheet might be viewed as an arrangement of superhelically coiled strands lying on the surface or adjacently packed cylinders (a). However, in order for any central chain (solid rod) to simultaneously conform to two local superhelix axes (dashed lines) the chains must be essentially straight helices, so producing the hyperbolic paraboloid shown in (b).

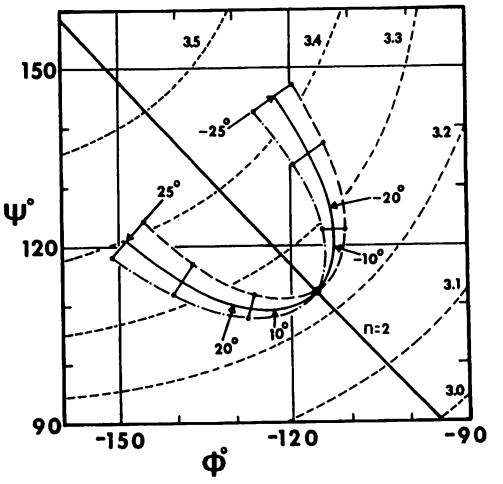

FIG. 9. A ϕ, ψ plot showing the conformational pathway for twisting a parallel β-sheet which optimizes the interchain hydrogen-bonds. The solid line describes structures composed of straight helical chains with all ϕ's and ψ's equivalent. The dashed lines describe how two strands twist to form coils with residues of alternating conformations (e.g. connected points on the curves). Coiled chains are found at the edges of some parallel sheets and in some β-barrels (Salemme and Weatherford, 1981a). Degree designations give interchain twist angle; short dashed curves give residue helical repeat (Fig. 3).

successive parallel strands are connected by α-helices packing on the exterior surface of the β-sheet cylinder (Fig. 5). The overall structure is therefore composed of an inner, typically eight-stranded β-barrel, surrounded by an external cylindrical array of eight nearly aligned α-helices. If the structure is unfolded about the barrel axis, it is clear that one difference between this and the generally observed saddle-shaped β-α-β domains is that the former have α-helices contiguously connecting sheet strands on the same (i.e. exterior) side of the sheet.

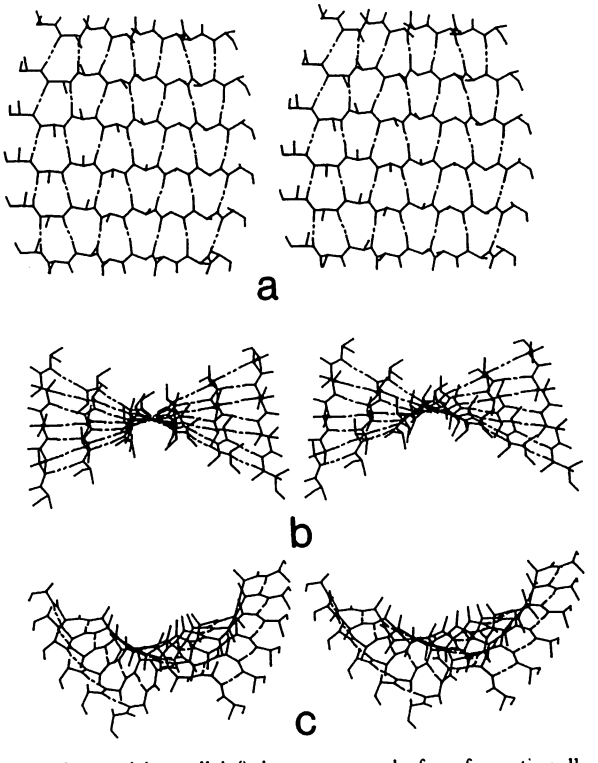

FIG. 10. Sterioviews of a model parallel β-sheet composed of conformationally identical, straight helical polypeptide chains.

Nevertheless, the difference in the final twisted geometry attained in the saddle-shaped vs cylindrical sheets more fundamentally reflects differences in the pattern of their interchain hydrogen-bonding. Barrel-forming sheets have staggered chains, so that their hydrogen bonding plans are rhombic instead of rectangular as in saddle-shaped sheets. As shown in Fig. 11, twisting the chains in a rectangular plan sheet results in an equivalent extent of chain divergence at the chain ends. Correspondingly, adjacent chains most closely approach each other along a line which bisects each of the sheet strands. The effects are similar in a rhombic plan sheet. However, owing to the staggered interactions in the rhombic sheet, twisting the chains results in the introduction of cylindrical curvature into the structure (Fig. 12). With increasing twist, such sheets can close to form surfaces which are hyperboloids of one sheet (Fig. 13). These cylindrical surfaces have a smaller diameter at the barrel equator where adjacent twisted chains most closely approach and diverge to larger diameters at the open ends of the cylinder. The overall geometrical properties of this structure manifest themselves in observed parallel β-barrels, where the chains are generally found to diverge at the barrel ends (Fig. 14). Interestingly, cyclic closure of the rhombic sheet seems to require a relatively unique pattern of staggered chain interactions, so that when the chains twist, the barrel can close with the hydrogen-bonds in proper register. Figure 15 illustrates a model eight-strand parallel barrel and the relationship of its hydrogen bond plan to that observed in the β-barrel in triose phosphate isomerase (Banner *et al.*, 1975).

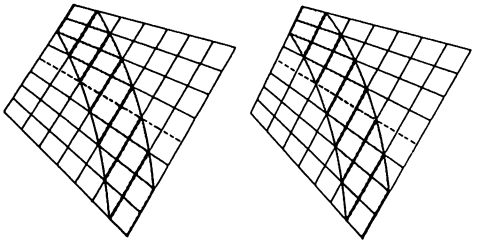

FIG. 11. Schematic view of a β-sheet of staggered plan projected onto a hyperbolic paraboloid. The heavy broken line indicates the line of isotropic stress distribution in the rectangular sheet. Truncation of the rectangular sheet wings upsets this balance of forces, so that the stress distribution is no longer uniform in the staggered sheet. As a result, staggered arrays spontaneously deform to surfaces having the cylindrical geometry of a hyperboloid of one sheet.

Despite the apparent differences between the spatial geometries attained by rectangular and rhombic plan parallel sheets, their final states reflect the same underlying compensations between chain twisting and constraints imposed by hydrogen-bond preservation. In fact, both of the surfaces formed by these sheets are well known to reflect a uniform distribution of forces in stressed membranes (Otto, 1969). For example, soap films (Boys, 1959) suspended from a twisted rectangular wire frame, or a pair of rings defining the ends of a cylinder, conform respectively to the hyperbolic paraboloid and hyperboloid of one sheet (Gellert *et al.*, 1977) characterizing twisted parallel β-sheets (Fig. 16).

2. *Antiparallel β-Sheets*

The spatial geometries of antiparallel β-sheets observed in proteins exhibit considerably more structural diversity than seen in parallel sheet structures. This is a consequence of several fundamental differences between the geometry of antiparallel and parallel sheets. The net consequence is to endow antiparallel sheets with greater conformational flexibility which allows them to accommodate a greater variety of twisted states while still preserving good interchain hydrogen bonds. A primary difference distinguishing the antiparallel and parallel structures is reflected in the ability of the former to assume different flat conformations. While the preservation of good hydrogen-bonds between the chains of a parallel sheet is associated with a particular polypeptide chain conformation on the ϕ, ψ plot, the classical antiparallel structure with linear N-H-O-C′ hydrogen-bonds is one of many such possibilities (Fig. 17). Owing to the symmetry of the antiparallel sheet, it can achieve a continuum of flat

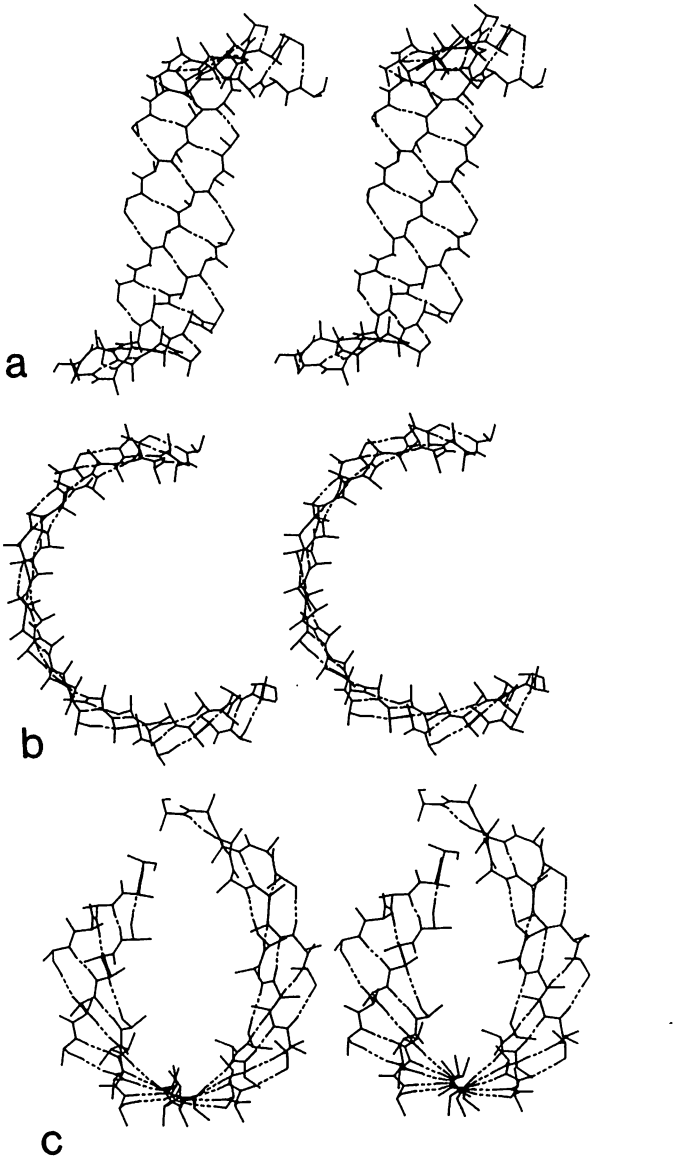

FIG. 12. Stereoviews showing the results of optimizing interchain hydrogen-bonds between straight helical chains arranged in a staggered plan. Owing to the combination of interchain twist and rise, a cylindrical surface results.

conformations, all lying on the $n=2$ line of the ϕ, ψ plot. These alternative conformations reflect continuous variation of the chain dipeptide repeat period and an associated isoenergetic bending of the hydrogen-bonds at the carbonyl oxygens (Hagler *et al.*, 1974). As described below, this ability of the antiparallel structure to alter its extension while still preserving its hydrogen bonds is a principal factor leading to geometrical diversity in twisted antiparallel sheets.

In contrast to parallel β-sheets which typically form an internal structural backbone in proteins, antiparallel sheets are generally found to form exterior surfaces of domains or globular proteins. When antiparallel sheets are situated internally, it is usually the consequence of the association of antiparallel β-domains within a globular protein, or a result of subunit packing within an oligomeric protein structure (Salemme and Weatherford, 1981b). In situations where rectangular-plan antiparallel sheets do occur at internal interfaces in proteins (Fig. 18), they may approximate saddle-shaped surfaces composed of straight helical chains (Fig. 19). Alternatively, antiparallel strands may be incorporated into

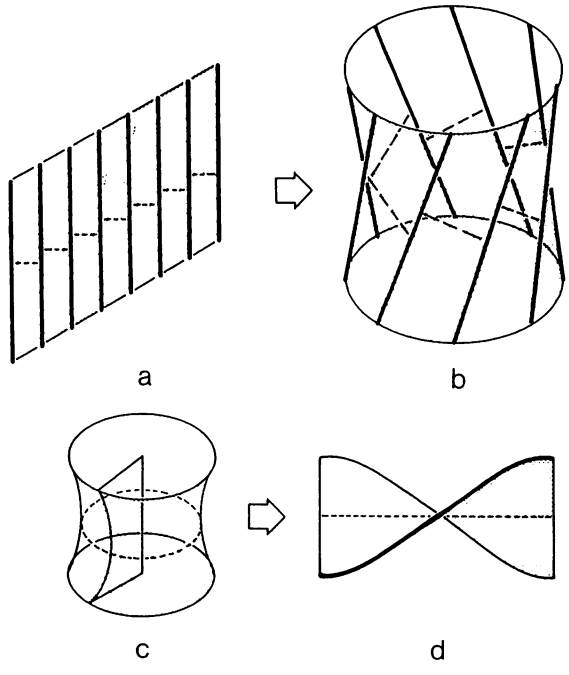

FIG. 13. (a) A plan view of a staggered β-sheet indicating the (broken) lines of symmetrical stress distribution (or interchain closest approach) when the structure is twisted. As shown in (b), twisting results in the formation of a catenoid of hyperboloid of one sheet, an anticlastically curved, isotropically stressed surface that results from the combination of interchain twist and rise in the staggered plan sheet. As noted by Boys (1959), a catenoid surface may be cut along a radial plane (c) and opened to produce a helicoid surface (d)

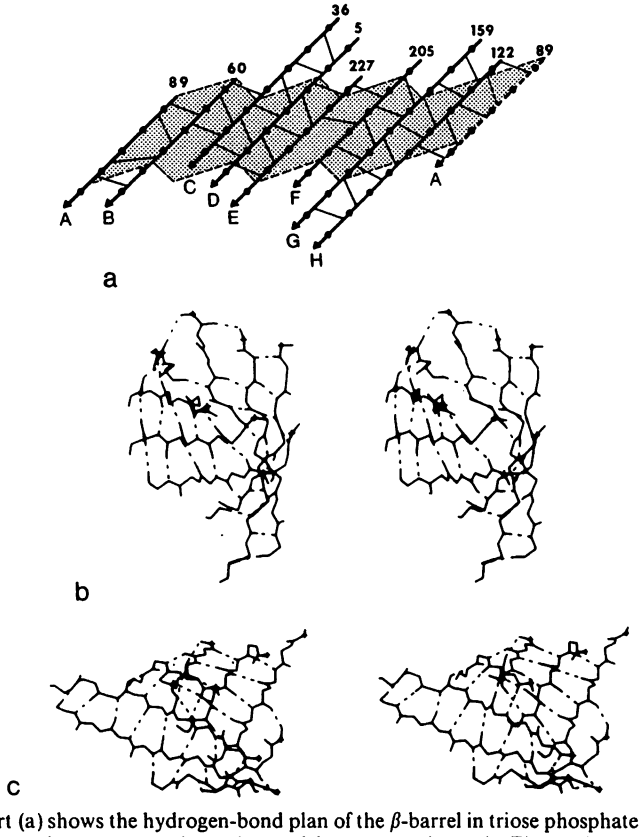

FIG. 14. Part (a) shows the hydrogen-bond plan of the β-barrel in triose phosphate isomerase, where the shaded overlay corresponds to the model structure shown in Fig. 15. Parts (b) and (c) show stereoviews of the structure (Feldmann, 1976) illustrating the divergence of the sheet strands at the barrel ends.

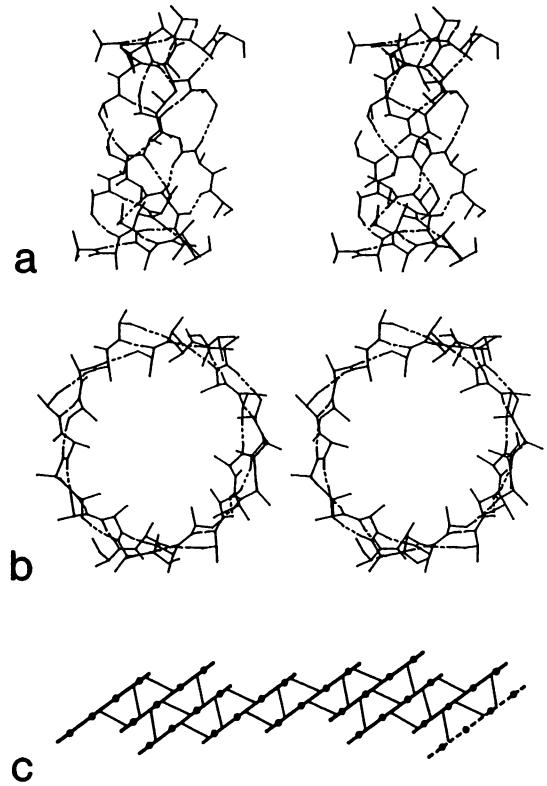

FIG. 15. Stereoviews ((a) and (b)) of a conformationally regular eight-strand barrel composed of straight helical chains. Part (c) illustrates the hydrogen-bonding plan.

more extended multiple strand parallel sheets to form a mixed parallel–antiparallel sheet. In the latter case it is notable that owing to their variable repeat period, the antiparallel chains of the sheet can assume conformations which allow good registration between the parallel and antiparallel sections of the sheet (Salemme and Weatherford, 1981b) (Fig. 20). The structural properties of these internal, antiparallel or mixed sheets are therefore determined by the same factors operative in rectangular plan parallel sheets. However, the great majority of antiparallel sheets in proteins exhibit more complex curvatures. This is a result of both the variable extensibility of the antiparallel structure and the quite different nature of the geometrical constraints imposed by hydrogen bonding when antiparallel sheets twist.

In contrast to the parallel sheet, the polypeptide chains of a *double-strand* antiparallel sheet can twist in a manner which completely preserves the integrity of the interchain hydrogen-bonds (Fig. 21). This twisting behavior involves different, but correlated changes in the ϕ, ψ conformational angles of residues situated in the "small" and "large" hydrogen-bonded rings of the double-strand sheet structure. The twisted structures produced are double helices whose *coiled* polypeptide chains are composed of dipeptide repeating units (e.g. one "small" and one "large" ring residue) (Raghavendra and Sasisekharan, 1979; Salemme and Weatherford, 1981b; Chothia, 1983). The fact that any sterically accessible double-strand flat sheet (Fig. 17) can coil with the perfect preservation of the hydrogen-bonds is a primary reflection of the enhanced flexibility of the antiparallel sheet vs the parallel structure. Whereas double strand parallel sheets occur only rarely in proteins, double strand antiparallel sheets are relatively common. In general these are high twisted double-helical arrangements (Fig. 22), which may nevertheless correspond closely to regular model structures (Fig. 23). As discussed in Section IV, the observed highly twisted arrangement is a result of both chain conformational effects and favorable packing among amino-acid side-chain residues. Consequently, the formation of these double helical coiled structures reflects the participation of hydrogen-bonding, conformational and packing forces acting in concert.

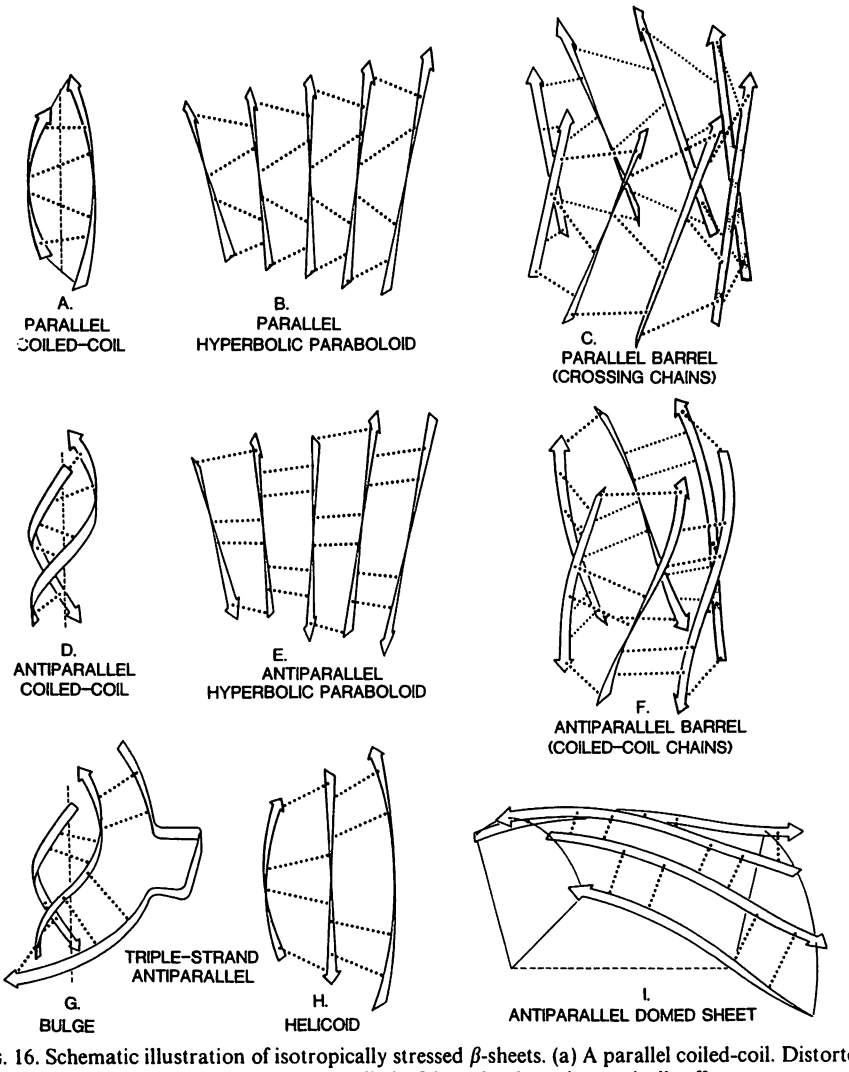

FIG. 16. Schematic illustration of isotropically stressed β-sheets. (a) A parallel coiled-coil. Distorted versions of this arrangement occur principally in β-barrels where they typically effect some extent of local curvature required to close the structure. (b) A parallel hyperbolic paraboloid composed of straight helical crossing chains. (c) A parallel barrel made of a staggered array of straight-helical crossing chains. Observed structures typically have more extensive interchain hydrogen-bonding than is compatible with the extensive twisting required for closure, and so incoporate conformational or hydrogen-bonded irregularities and local regions of coiled-coil conformation. (d) A double-strand antiparallel coiled-coil that can occur in many variations and can be much more extensively twisted than the parallel double strand structure. (e) Antiparallel hyperbolic paraboloid. Regular configurations are relatively infrequently observed owing to the conformational flexibility associated with the interchain hydrogen-bond geometry, which allows them to be readily deformed in response to extended packing instructions. (f) An antiparallel barrel composed of coiled-coil chains. Observed structures typically have more extensive interchain hydrogen-bonding than is compatible with the twist required for closure. Consequently, they both depart from true cylindrical geometry and incorporate various conformational and hydrogen-bonding defects resulting from the extensive twist of the polypeptide chains. (g) A triple strand antiparallel structure with a β-bulge. The bulge results from the inability of the third strand to conform to the highly coiled double-strand structure. (h) Shows an alternative triple strand helicoid sheet (Fig. 13(d)). (i) An idealized antiparallel, domed sheet composed of slightly twisted coiled-coils that obey a common (broken line) superhelix axis. Further discussion is given in the text.

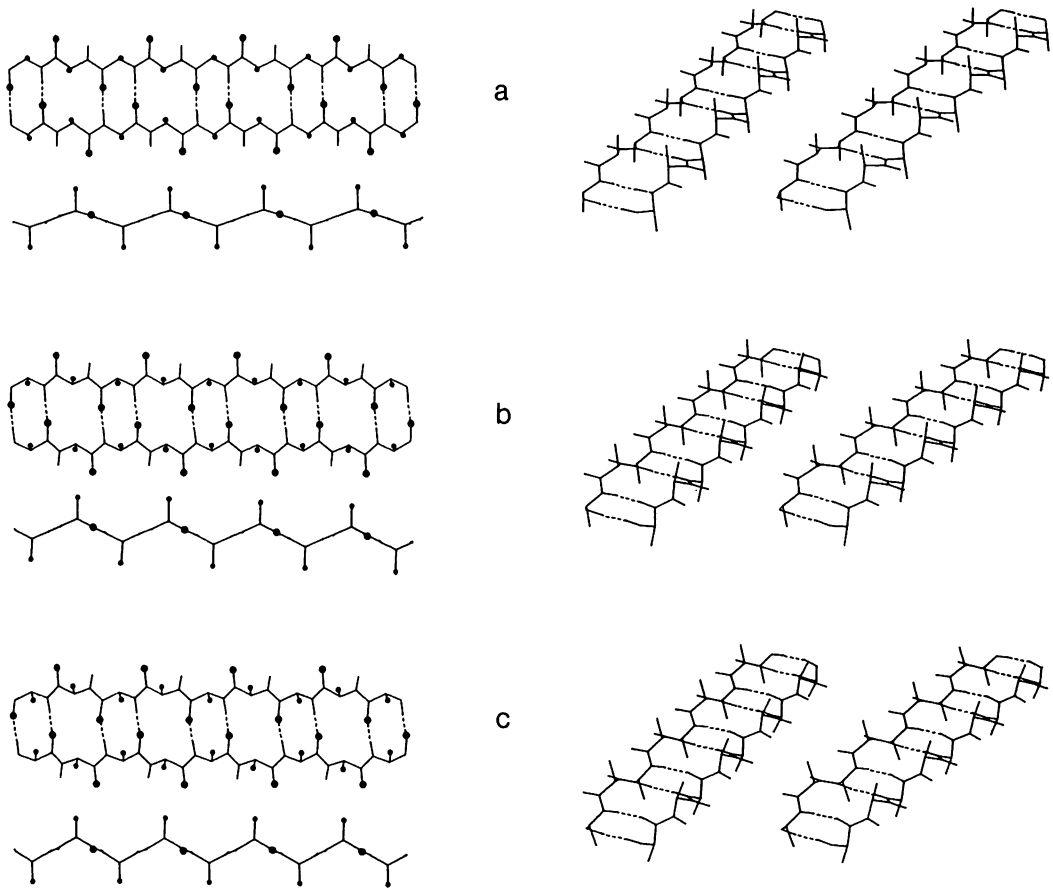

FIG. 17. Views of flat antiparallel β-sheets illustrating variations in polypeptide chain repeat and NOC′ hydrogen-bond bend angle.

This situation contrasts to virtually all other β-sheet arrangements where the extent of chain twist is ultimately constrained by the interchain hydrogen-bonding interactions.

Although hydrogen-bonding interactions constrain the extent of twist in antiparallel sheets of three or more chains, many antiparallel sheets manifest incorporation of coiled polypeptide chains. For example, contiguous triple strand sheets of roughly rectangular plan occur as subdomains in some globular proteins (Fig. 16(h)) (Salemme and Weatherford, 1981b). In these structures the central chain approximates a simple helical polypeptide, while the two edge strands are helical coils lying on a cylinder whose axis is defined by the central chain (Fig. 24). The attainment of this arrangement reflects the tendency of the exterior antiparallel strands to coil, together with their ability to adjust their polypeptide chain period to accommodate the hydrogen bond period of the central chain.

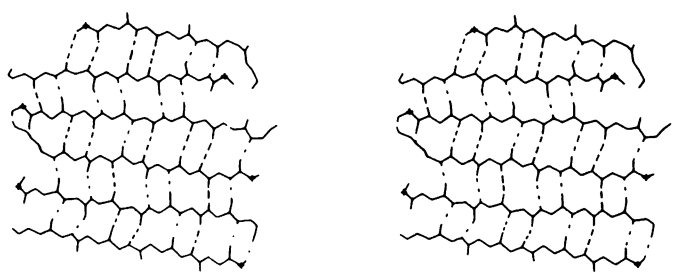

FIG. 18. Stereoview of the extended interior antiparallel sheet in concanavalin A (Feldmann, 1976).

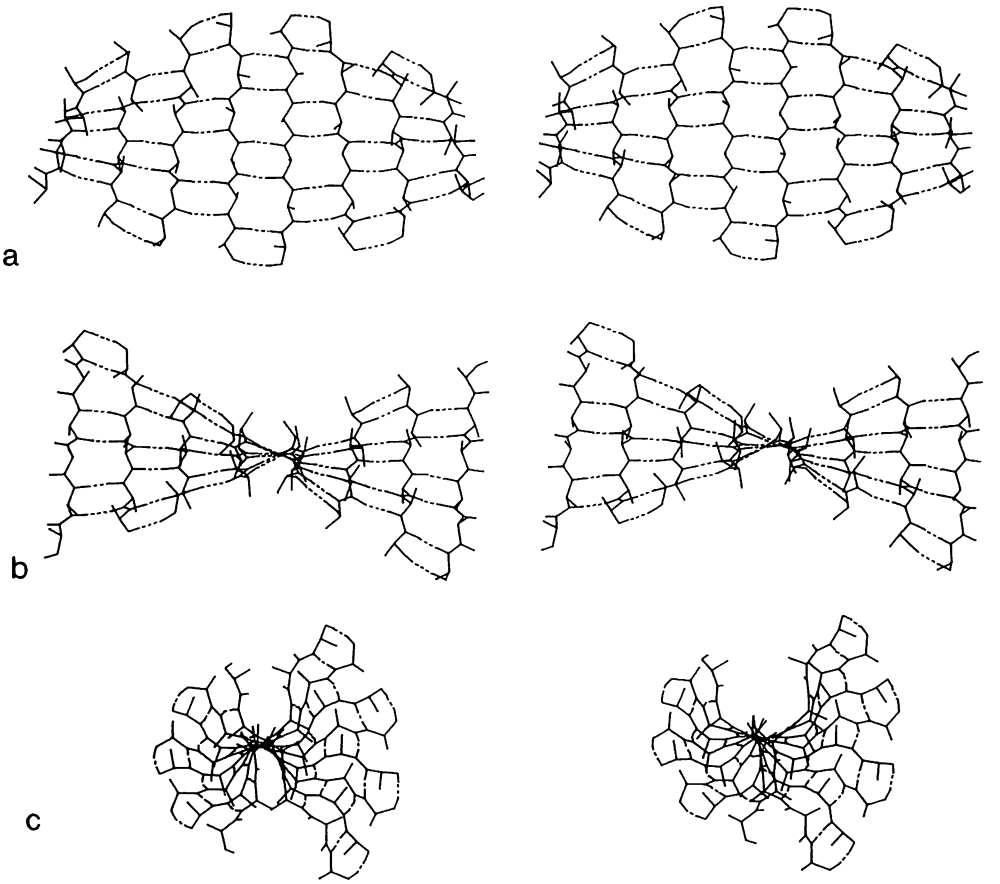

FIG. 19. A model antiparallel sheet composed of straight helical polypeptide chains. Relatively many straight helical conformations can produce such sheets owing to the variable period properties of the antiparallel sheet (Fig. 17).

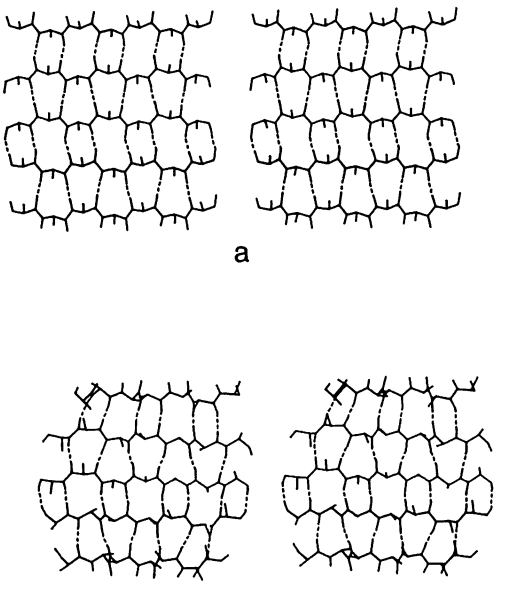

FIG. 20. Part (a) shows a flat mixed β-sheet where the chain conformation in the antiparallel strands required to produce good interchain hydrogen-bonds is sterically unfavorable (Salemme and Weatherford, 1981b). Twisting the sheet (b) tends to alleviate these constraints because the parallel chain period becomes more extended when sheet twists (Fig. 9).

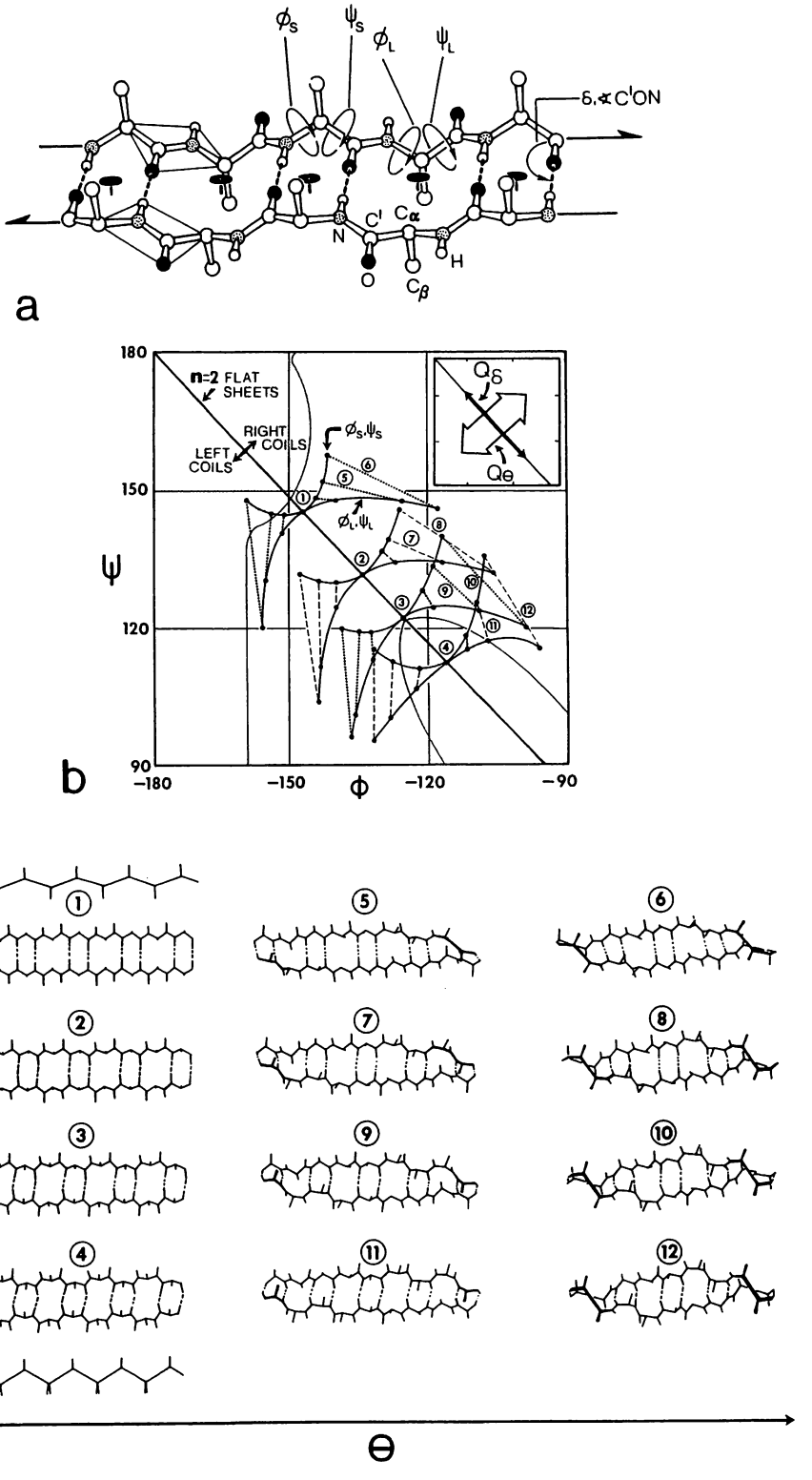

FIG. 21. Coiling in double strand antiparallel sheets. Part (a) illustrates the conformational degrees of freedom in the structure; the ϕ's and ψ's of the small and large hydrogen-bonded rings, and hydrogen-bond bend angle δ, which varies with the chain helical repeat period (Fig. 17). Part (b) shows coupled ϕ, ψ trajectories for coiling the sheets from representative flat structures. Numbered pairs of ϕ, ψ conformations in (b) correspond to structures shown in (c). Cooperative ϕ, ψ displacements in the sheet can be viewed as essentially independent vibrational modes ($Q\delta$ and $Q\theta$, inset, part (b)) which are superimposed to produce the structures shown in part (c).

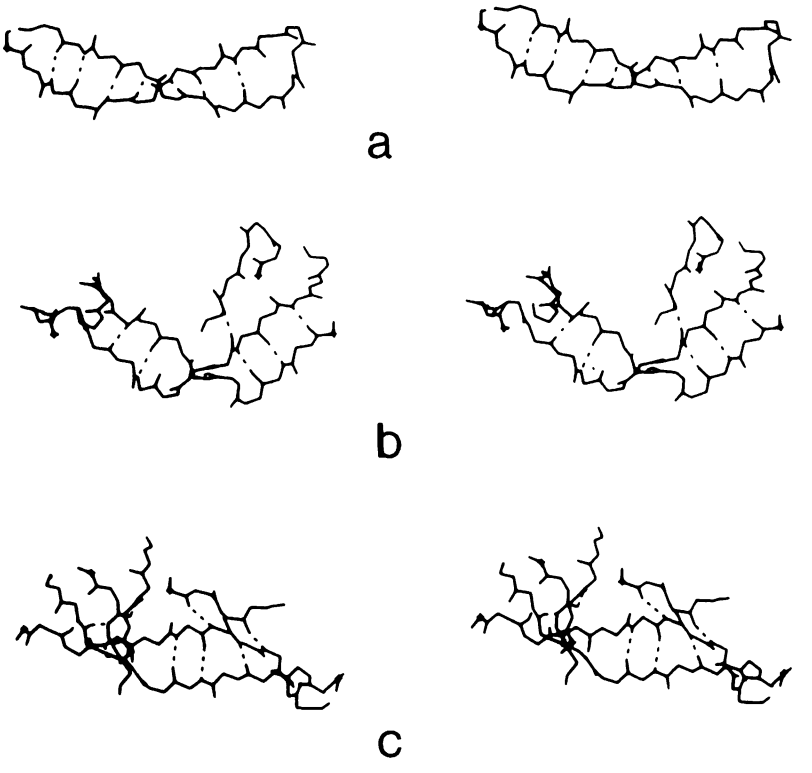

FIG. 22. Examples of double-strand antiparallel coils in proteins. (a) Pancreatic trypsin inhibitor, (b) lactate dehydrogenase, (c) thermolysin (Feldmann, 1976).

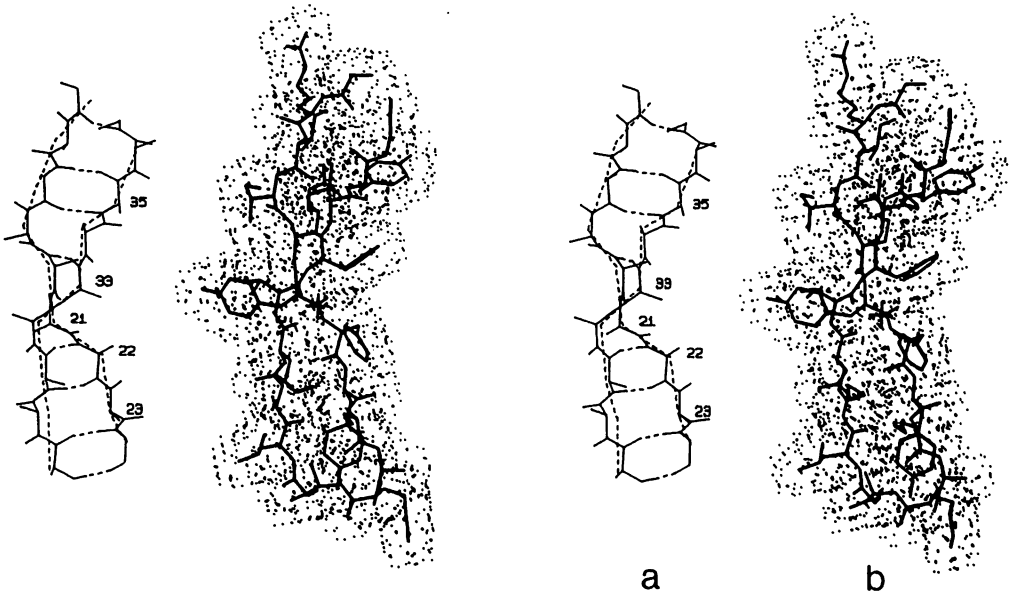

FIG. 23. (a) A least squares superposition of a regular antiparallel coiled-coil with $\phi_s = -114°$, $\psi_s = 150°$, $\phi_L = -92°$, $\psi_L = 114°$, $\delta = 163°$ (unbroken lines) with the α-carbon positions of the double-strand β-sheet (broken lines) in pancreatic trypsin inhibitor. The average superposition error in model vs observed C_α coordinates is 0.52 Å. (b) A pseudo-space-filling representation of the trypsin inhibitor β-coil illustrating the intimate side-chain packing attained in this strongly twisted conformation.

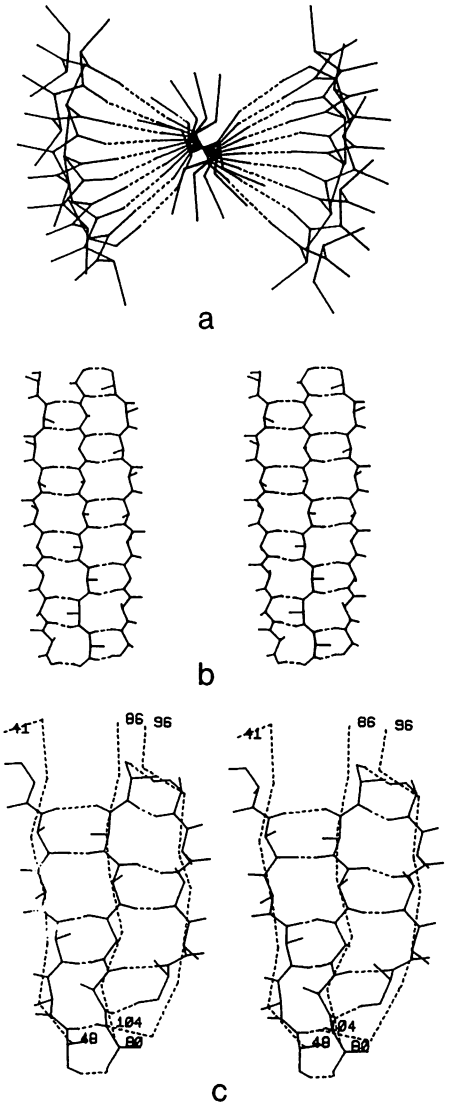

FIG. 24. Axial (a) and stereoscopic (b) views of a triple strand antiparallel model with a straight helical central chain and coiled peripheral chains (see Figs 13 and 16(h)). Part (c) shows a least squares fit of a regular model (solid lines) to a region of triple strand helicoid-sheet in ribonuclease (Salemme and Weatherford, 1981b).

In principal, it might be assumed that coiled antiparallel chains would lend themselves to the formation of multiple strand β-barrels with staggered chains (Fig. 16(f)). That is, the tendency of the chains to coil could allow each chain to truly conform to a cylindrical barrel surface. While this added chain flexibility does seem to be reflected in observed smaller radii (i.e. fewer strands) of antiparallel vs parallel barrels, antiparallel barrels nevertheless appear to share the divergence at the barrel ends seen in the parallel sheets (Fig. 25). Modelling studies suggest that this reflects the introduction of cummulative hydrogen-bonding constraints in the extended antiparallel structures which prevent the sheets from attaining the coiled conformations required for formation of a regular barrel. In fact, observed barrel structures typically incorporate chains of non-uniform twist, a situation which reflects the inability of the chains to conform to the geometrical requirements for closure of the barrel. Additionally, particularly tight-radius changes in curvature which are incompatible with regular hydrogen-bonding in a continuous sheet, are accommodated by the introduction of a bulge residue in the β-structure (Richardson *et al.*, 1978). This has the effect of relieving the local geometrical constrains imposed by the introduction of the twist required for closure,

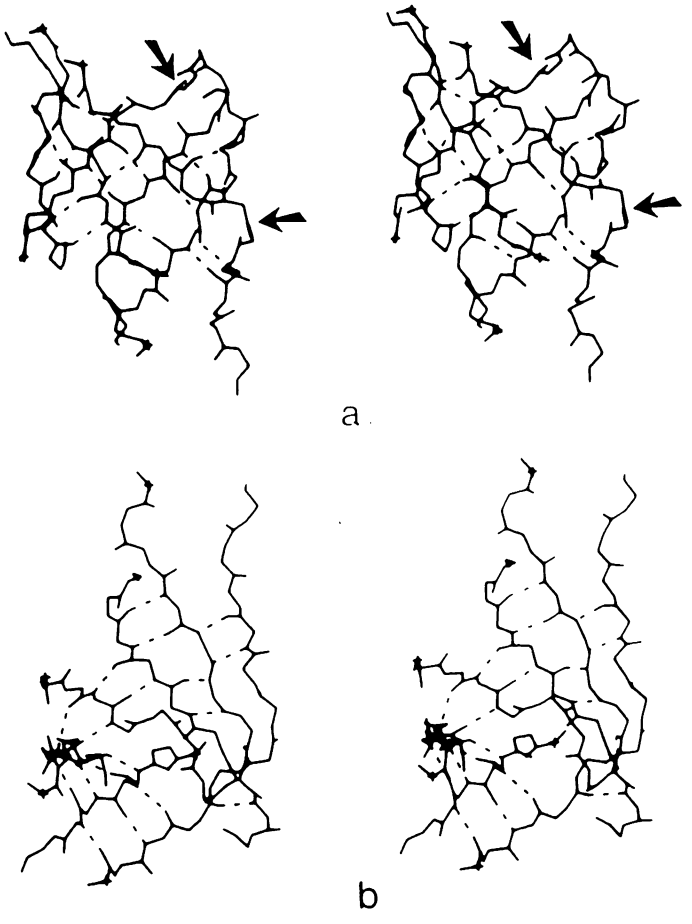

FIG. 25. The amino-terminus antiparallel β-barrel in α-chymotrypsin (Feldmann, 1976). The most extensively hydrogen-bonded regions of this structure can be viewed as locally distorted arrangements of either of the idealized triple strand structures shown in Fig. 16(g) and (h). Note that closure of the structure requires the introduction of strong localized interchain twists that produce bulges (arrows). The view shown in (b) emphasizes the divergence of the chains towards the ends of the barrel, which reflects the limitations in the twist that may be accommodated in antiparallel coiled sheets.

while generally preserving the continguous hydrogen-bonding in the sheet (Figs 16(g) and 25).

Although many staggered plan antiparallel sheet structures occur in observed protein structures, they tend to progressively deviate from cylindrical geometry as the sheets get larger (Fig. 16). Instead, several of the intermediate-size sheet structures form arrangements which, although "topologically" similar to the classical β-barrels, appear more as a pair of interconnected, stacked β-sheets (Richardson, 1981; Cohen *et al.*, 1981; Chothia and Janin, 1983). This presumably reflects effects of the extended hydrogen-bonded interactions within each subsheet, which introduce constraints that prevent the extent of chain coiling required for barrel formation. Instead, two curved sheets pack together to form a flattened "sandwich" arrangement. However, these and larger sheets which occur in proteins frequently manifest the incorporation of coiled polypeptide chains (Salemme and Weatherford, 1981b; Chothia, 1983) (Figs 26 and 27). The constraints on sheet twist which arise as the structure becomes more extended are particularly apparent in the β-sheet of bacteriochlorophyll binding protein (Matthews *et al.*, 1979) (Fig. 27). Here the wings of the sheet, which incorporate staggered chains, exhibit a smooth curvature reflecting its composition by coiled polypeptide chains. However, the central region of the sheet, where there are extensive cross-chain interactions, is essentially flat.

Summarizing, observed antiparallel sheets exhibit a much greater variety of geometrical

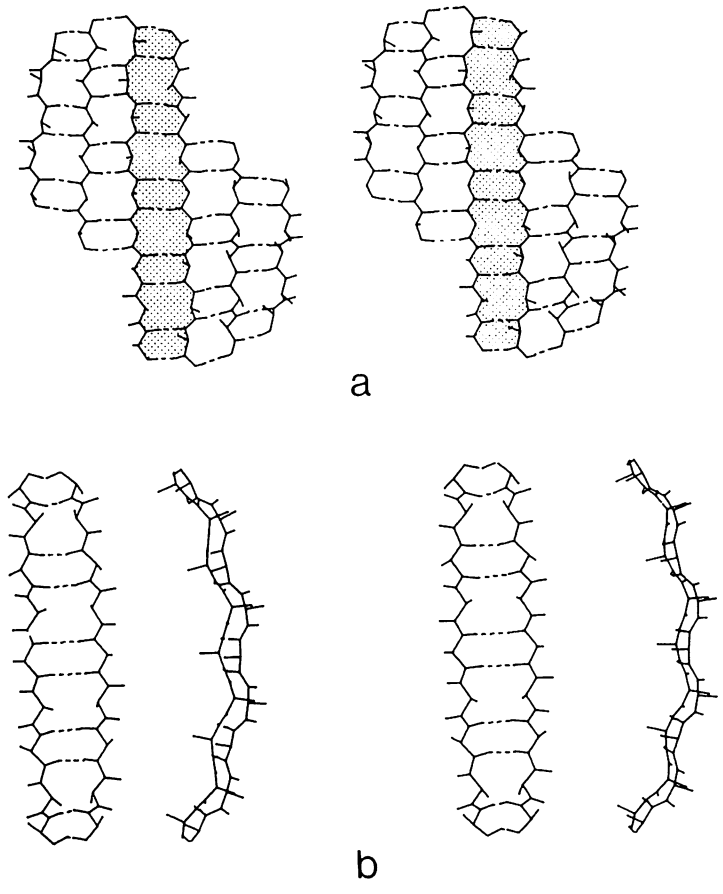

FIG. 26. (a) An extended antiparallel β-sheet composed of identical coiled chains. The introduction of more extensive curvature into such structures necessitates that the outer strands of such arrays assume more extended coiled-coil conformations, which will generally result in an arrangement having a continuously varying curvature. (b) Some continuously deformed β-sheets exhibit sheet curvature that apparently reflects the effects of extended packing forces that tend to bend the sheet (see, e.g. Fig. 27(b)). Bending the sheet so that its polypeptide chains lie on a cylindrical surface whose major axis lies perpendicular to the chain directions causes the chains to untwist and the interchain hydrogen-bonding to become somewhat poorer relative to more twisted, but less bent, coiled conformations. Note that bending the double strand sheet situates the "small ring" C_β residues on the concave sheet surface.

configurations and chain conformations than seen for parallel structures. This reflects both the ability of antiparallel chains to coil and alter their dipeptide repeat periods. Taken together, these features endow the extended structures with considerable flexibility.

IV. THE ENERGETICS OF β-SHEET TWISTING

The foregoing studies of β-sheet geometry examined the consequences of twisting a regular lattice structure subject to boundary constraints imposed by the interchain hydrogen-bonds. These studies treated the tendency for the polypeptide chain to twist in an *ad hoc* fashion. That is, different twisted structures were evaluated by generating polypeptide chains with various helical conformations, and then testing their ability to assemble in ways which preserved optimally equivalent interchain hydrogen-bonds (Salemme and Weatherford, 1981a,b). The approach was based on an analysis of the conformational potential energy for a single polypeptide chain. Depending on the specific nature of the potential function used, these typically show a broad potential energy minimum in the extended region of the ϕ, ψ plot, which corresponds to a locally left-handed helical conformation (Ramachandran, 1974; Raghavendra and Sasiekaharan, 1979). To a first approximation, this result seems sufficient to explain the observed twist in β-sheets, since only extended polypeptide chains are compatible with the formation planar hydrogen-bonded arrays. On the other hand, it might

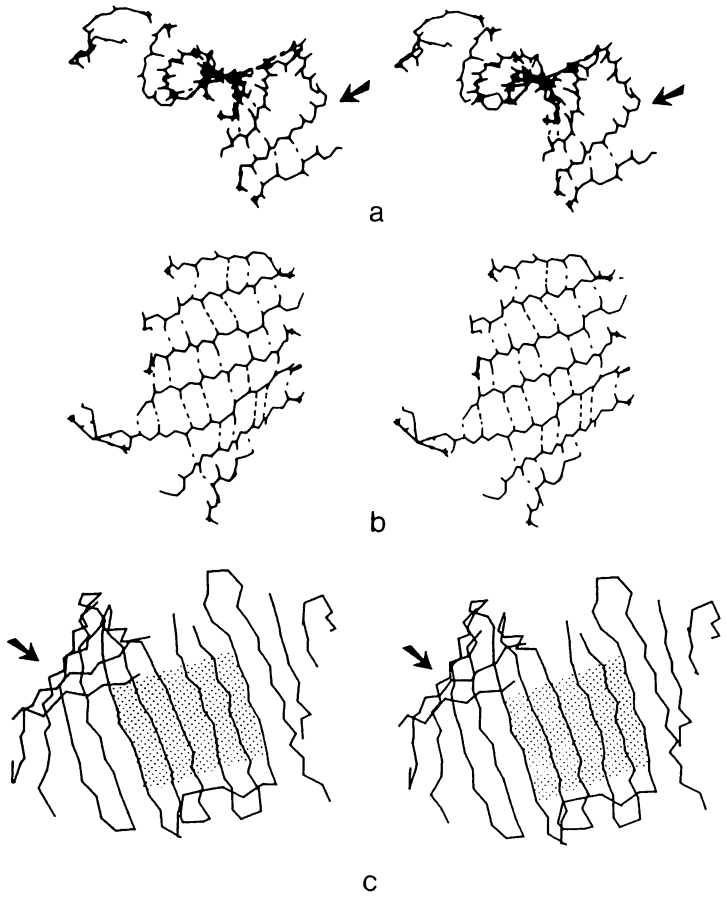

FIG. 27. Examples of continuous deformations in antiparallel β-sheets. (a) A region of the antiparallel β-sheet in glyceraldehyde-3-phosphate dehydrogenase (Feldmann, 1976). The central strands of this structure have slight coiled-coil character giving the overall sheet apparent cylindrical curvature (Fig. 16(i)). Note that one outer strand contains a bulge (arrow), presumably owing to the inability of this strand to become both sufficiently extended and maintain the geometry required for regular hydrogen-bond formation to the inner coiled-coil strands (*cf.* Fig. 16(g)).

(b) The exterior antiparallel β-sheet in concanavalin A (Feldmann, 1976). This sheet is composed of coiled chains that appear to have become untwisted in the central region, in response to different packing interactions on opposite sides of the sheet, which cause it to bend about a cylindrical axis at right angles to the direction of the polypeptide chains (see Fig. 26).

(c) The β-sheet in bacteriochlorophyll binding protein (Bernstein *et al.*, 1977). The shaded overlay shows the region of this sheet which is essentially flat, presumably owing to the extensiveness of the regular hydrogen-bonding both along and across the sheet in this region. The staggered region of the structure (arrow) exhibits continuous curvature that results from the structure's chains taking on slight coiled character. The structures shown here manifest the continuously deformable properties inherent in extended antiparallel β-sheets.

be anticipated that non-bonded interchain interactions could additionally play a significant role in the stabilization of twisted β-sheets. Similarly, such interactions could compensate for, or result in, larger hydrogen-bond deformations than apparent from the geometrical modelling studies. Specifically, the geometrical studies assumed that the preservation of interstrand hydrogen-bonds was the determinative factor governing twisted sheet geometry. The close correspondence between the observed and geometrically modelled structures (typically less than 1.0 Å for all backbone atoms) justifies this approach as an accurate initial approximation to the physical situation (Salemme and Weatherford, 1981a,b). Nevertheless, as the potential functions governing hydrogen-bond deformations may be somewhat "softer" than the effective potential utilized in the modelling studies (Hagler *et al.*, 1979), it is of interest to consider the energetics of sheet twisting in more detail.

A straightforward approach to this problem might simply involve a potential energy

minimization of a flat β-sheet to produce the corresponding minimum energy twisted structure. However, attempts to do this typically encounter a familiar difficulty common to most *ab initio* protein folding computations; the structure becomes trapped in a local minimum long before the structure reaches the global minimum associated with the observed structural geometry. Chou *et al.* (1982) consequently approached the problem in a manner similar to that used in the geometrical modelling studies. These authors focussed attention on extended β-sheet structures composed of straight helical polypeptide chains (i.e. corresponding to saddle-shaped sheet surfaces, Fig. 7). They assembled both parallel and antiparallel chains of various helical conformations in a fashion similar to that utilized in the geometrical studies, but evaluated the potential energy of the resulting structures using a full interatomic potential set, rather than the simple hydrogen-bond optimization used in the geometrical modelling. They arrived at the following conclusions concerning the energetics of twisted sheets composed of straight helical polypeptide chains. (1) In virtually all cases examined it was found that the most energetically favorable structure corresponded to a sheet with right-handed twist (as observed). The principal factor stabilizing the twisted conformations arise from *intrastrand* interactions in polypeptide chains composed of L-amino acids. Minimum energy polyalanine sheets, while twisted with the proper sense, were observed to have considerably less twist than seen in observed structures. However, studies of polyvaline sheets, an amino acid occurring frequently in β-sheets (Lifson and Sander, 1979), produced more twisted minimum energy structures which correspond more closely to observed sheets. Although intrastrand interactions were still a determinative factor in twisting polyvaline sheets, interstrand interactions appear to play an increasingly larger role in β-sheet stabilization for sheets with side chains larger than alanine. (2) Twisting the sheets was invariably associated with the progressive deformation of the interchain hydrogen-bonds. Minimum energy structures consequently manifest less twist either as the number or length of the sheet polypeptide chains increased. This behavior corresponds to results obtained from the geometrical lattice modelling of these structures. (3) Minimum energy conformations for parallel sheets were found to be more conformationally restricted than for antiparallel sheets. This suggests that antiparallel sheets are potentially more flexible than parallel sheets, a conclusion consistent with both the lattice modelling results and observation.

Although both parallel and antiparallel sheets are observed to form arrangements composed of straight-helical polypeptide chains, antiparallel sheets form such structures relatively rarely. As described in Section III, this is a manifestation of both the flexibility of the antiparallel structure and its symmetry properties which allow the formation of sheets incorporating coiled polypeptide chains. The energetic analysis of such sheets poses a formidable problem as many observed structures reflect a continuum of polypeptide chain conformations (Fig. 27). Consequently, symmetry based approaches incorporating the assumption that the sheet chains are conformationally equivalent are not readily applicable. Nevertheless, observed *double-strand* antiparallel sheets in proteins can form highly regular and symmetric double-helical arrangements (Fig. 23). Results of the geometrical modelling studies suggested that double-strand antiparallel coils were potentially structures of extraordinary flexibility. This is a consequence both of the symmetry properties of the structure, which allow equivalent preservation of all hydrogen-bonds when the structure coils, and the lack of boundary constraints because the sheet has only two polypeptide chains (Salemme and Weatherford, 1981b). Recent work in the author's laboratory has focussed on the energetics of double-helical coiling in antiparallel sheets. The objective was the determination of the potential energy surface associated with the continuous interconversion of various coiled structures as shown in Fig. 21. The results of the geometrical studies indicate that any of a continuum of flat structures can cooperatively coil to form double-helical structures. Coiling from a given flat conformation involves correlated, but different alterations of the ϕ, ψ conformations of residues situated in "small" and "large" hydrogen-bonded rings of the structure. As illustrated in Fig. 28, the coiling behavior of any double strand sheet can be viewed as a superposition of more primitive cooperative alterations of the structure as a whole. As illustrated, these cooperative alterations can be uniquely associated with corresponding vectorial displacements on the ϕ, ψ plot. As these vectorial displace-

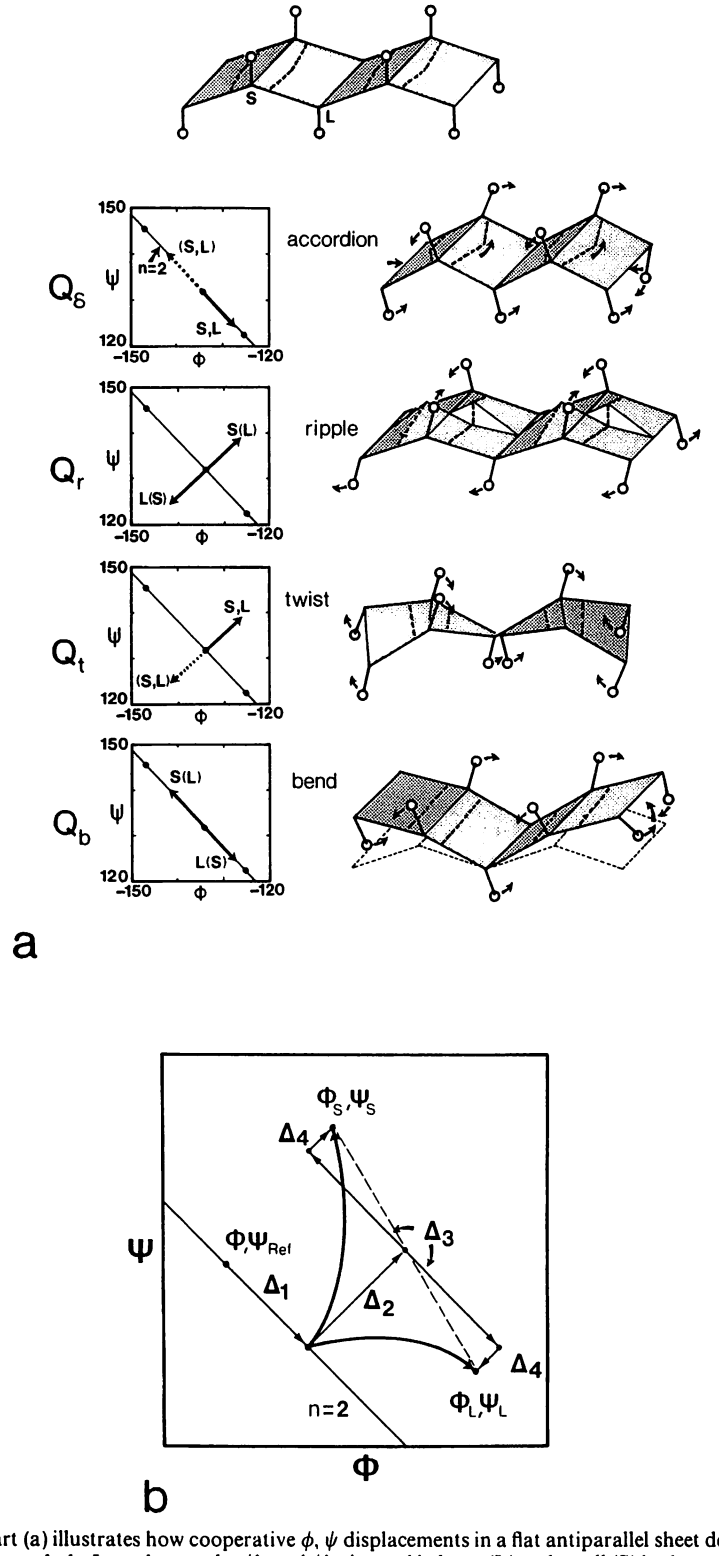

FIG. 28. Part (a) illustrates how cooperative ϕ, ψ displacements in a flat antiparallel sheet deform the structure as a whole. In each case, the ϕ's and ψ's situated in large (L) and small (S) hydrogen-bonded rings move along trajectories either coincident with or perpendicular to the $n=2$ line of the ϕ, ψ plot. For example, the accordion motion involves a correlated displacement of both large and small ring ϕ, ψ values along the $n=2$ line, while bend involves the conformations of S and L residues moving in opposite directions on the $n=2$ line, relative to an initial flat conformation. Twist and ripple are similarly related. Part (b) illustrates how the ϕ, ψ trajectories followed by the residues of a coiling β-sheet can be resolved as a superposition of the cooperative deformations shown in part (a).

ments constitute an orthogonal basis set, any coiled arrangement can be expressed as an expansion in terms of the vectorial ϕ, ψ displacements, e.g.

$$(\phi, \psi)\text{coil} = (\phi, \psi)_{FR} + \Delta_1(\phi, \psi)_A + + \Delta_2(\phi, \psi)_T + + \Delta_3(\phi, \psi)_B + \Delta_4(\phi, \psi)_R;$$

where $(\phi, \psi)_{FR}$ are the values associated with a flat reference structure, and the Δ_i's are scaling coefficients giving the relative magnitudes of the vectorial displacements and associated cooperative deformations shown in Fig. 28. Results of geometrical studies indicate that a continuum of flat structures lying on the $n=2$ line of the ϕ, ψ plot can cooperatively coil, so that the magnitude of the accordion-like displacements ($\Delta_1(\phi, \psi)_A$) which alter chain period constitute an independent variable in the production of coiled structures. On the other hand, when a given flat structure coils, maintenance of the interchain hydrogen bonds will correlate the values of Δ_3 (bend) and Δ_4 (ripple) with Δ_2 (twist). The potential energy surface for coiling these structures was therefore investigated by an iterative scheme which independently varied Δ_1 and Δ_2, and determined associated values of Δ_3 and Δ_4 corresponding to a minimum potential energy for the coiled structure as a whole. This treatment removes any *a priori* assumptions concerning preferred interchain hydrogen-bonding geometry, as the relative energies of the various assembled structures are evaluated using an all-atom interaction potential set (Momany *et al.*, 1975).

Figure 29 illustrates the behavior of some representative sections of the potential energy surface for double-helical coiling of polyalanine chains. Although a more complete

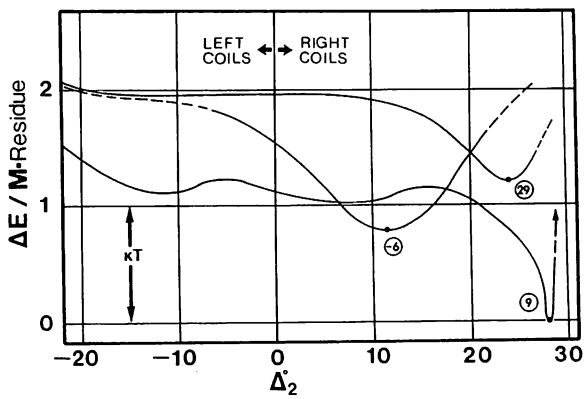

FIG. 29. Potential energy surfaces for coiling polyalanine double-strand antiparallel β-sheets. Relative energies in units of KT/mole amino acid residue (the structures are infinitely periodic double helices) are plotted as a function of twist displacement (Δ_2, Fig. 28) for structures with different extents of period variation (Δ_1, accordion, Fig. 28). The values −6, 9 and 29 give the lengths of the accordion vector displacements (with scalar magnitudes corresponding to degree increments on the ϕ, ψ plot) of each set of coiled structures relative to a reference flat structure with $\phi = -147°$, $\psi = 145°$.

description of this potential surface behavior will be given elsewhere, several features are of interest in the current context. Although the various flat structures themselves vary in energy (Chou *et al.*, 1982) it is in all cases true that structures with pronounced right handed coils have lower energies than left handed coils with comparable values of chain extension (Δ_1). On the other hand, the energies of coiled structures vary as a function of Δ_1, irrespective of the structure's coiling sense. Additionally, the rates of potential energy decrease with chain coiling (Δ_2), differ as a function of Δ_1. For example, there is little difference in energy between moderately left- and right-coiled structures with $\Delta_1 = 29°$, although a local minimum is reached at $\Delta_2 = 24°$. Thus, it may be that previous attempts to demonstrate an energetic preference of right- over left-coiled structures failed (Nishikawa and Scheraga, 1976) because they involved either comparisons of slightly coiled chains or alternatives with similar twists, but different chain periods. The different rates of potential energy decrease with Δ_1 reflect varying contributions of intra and interstrand interactions as the various structures coil. In general, contributions of intrastrand interactions become larger as Δ_1 tends towards 0 or negative values. However the local minima indicated on Fig. 29 reflect substantial

interstrand interaction components. This is apparent from inspection of the local minimum energy coil at $\Delta_1 = 9°$ (Fig. 30(a)), where it is clear that the highly twisted arrangement results in a compact interdigitating pattern between the alanine C_β carbons. Owing to the lack of boundary constraints on coiling the double-strand structure, the minimum energy configurations are generally more highly twisted than in multiple strand structures. Moreover, in fundamental contrast to the multiple strand structures whose twist is restrained by the deformation of the interchain hydrogen-bonds, both intra- and interchain interactions act in concert with the essential preservation of the hydrogen-bonds in stabilizing the coiled structures.

Viewing the coiling potential energy behavior as a three-dimensional surface, it is clear that the local minima on curves of differing Δ_1 values can be connected to form a low energy, c-shaped, valley. A structure undergoing an excursion along this valley would then undergo cooperative alterations in both coil twist and extension (Figs 21 and 30).

Studies of the potential surface behavior of polyvaline coils (KenKnight and Salemme, in preparation) show an overall qualitative similarity with the polyalanine results. The potential energy surface remains smoothly continuous, and both a global and a local continuum of minima occur which correspond to right-coiled structures. However, the

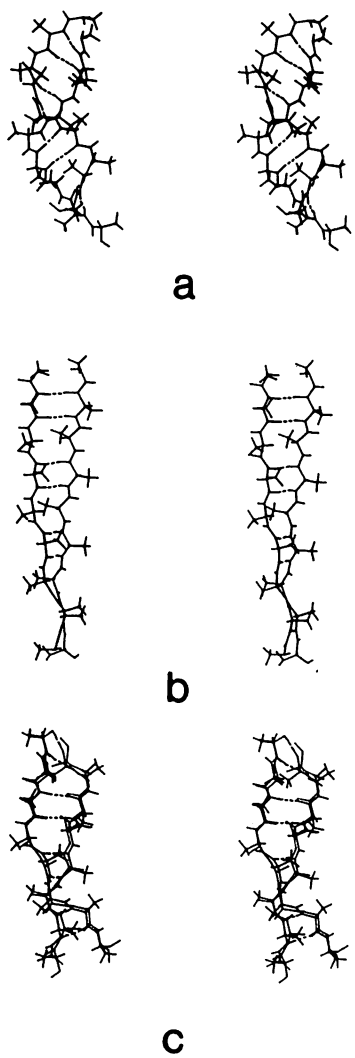

FIG. 30. Stereoviews of plyalanine minimum potential energy coiled structures. Structures correspond to minima shown in Fig. 29 at Δ_1 values of 9 (a), −6 (b), and 29° (c). The minimum energy structure shown in (c) is superimposed on the observed structural coordinates for the double-strand sheet in pancreatic trypsin inhibitor.

global minimum is shifted, and lies close to the local minimum for the polyalanine coil at $\Delta_1 = 29°$. This is a consequence of the fact that the C_β-branched valine residues cannot be sterically accommodated in the highly-twisted, polyalanine global minimum in Fig. 30(c). In fact, the $\Delta_1 = 29°$ minimum energy coil approximates the observed structure in pancreatic trypsin inhibitor with an RMS error 0.58 Å for the 64 corresponding backbone atoms.

Summarizing, the potential energy computations confirm the expectation (Salemme, 1982) that there exist a continuum of highly cooperative coiling trajectories for double strand β-sheets. The relatively slow variations in potential energy, associated with the cooperative motions that preserve the interchain hydrogen-bonds, are basic manifestations of the structure's flexibility. As described in Section V, this feature is of substantial interest with regard to both antiparallel β-sheet folding and stabilization in a dynamically active solvent environment.

V. CONFORMATIONAL REGULARITY IN β-SHEETS

Multiple stranded parallel sheets, composed of straight helical chains, and double strand antiparallel sheets, composed of coiled chains, represent two quite different structures which nevertheless share the property of conformational equivalence among their individual constituent polypeptide chains (Salemme and Weatherford, 1981a,b). In contrast, few if any of the corresponding observed structures exhibit this extent of conformational regularity. The observed deformations could potentially arise from the local optimization of intra- and interchain interactions which introduce corresponding localized deformations into the structure's long range regularity. Two different sorts of effects can be envisioned. Consider first a finite twisted sheet composed of homopolymer polypeptide chains. Although the side chain substituents are identical in such structures, the interchain interactions are not uniform throughout the sheet (e.g. the polypeptide chains tend to spatially diverge at the ends of saddle-shaped parallel sheets). As a result, the minimum energy configuration of the sheet will reflect the local optimization of side-chain packing interactions. This can, in turn, introduce local conformational irregularities into the polypeptide backbone. This is particularly true in small sheets, where the effects of extended hydrogen-bond interactions constraining the sheet to be regular are relatively relaxed. Chou and Scheraga (1982) (see also Chou *et al.*, 1982) investigated the magnitude of this effect by energy minimization of a conformationally regular twisted polyalanine sheet. They reported relatively small changes in the structure's energy and associated deviations in ϕ, ψ of about $\pm 3°$ relative to the conformationally regular structure. Deviations of this magnitude are substantially smaller than those typically observed on comparing crystallographically observed structures and their corresponding conformationally regular models (Fig. 31) (Salemme, 1981). However, it

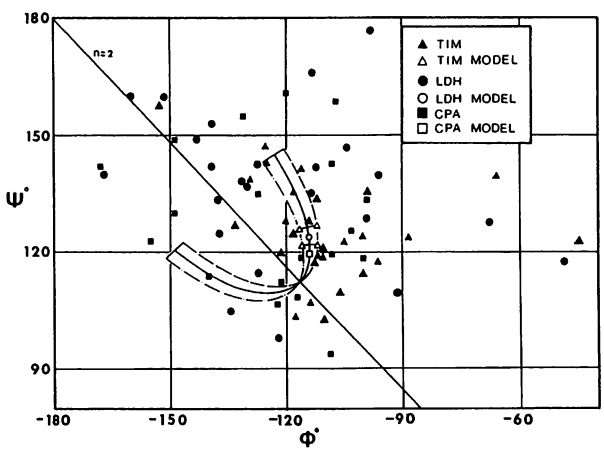

FIG. 31. A plot comparing observed conformational values for representative parallel β-sheet structures in triose phosphate isomerase (TIM), lactate dehydrogenase (LDH) and, carboxypeptidase A(CPA), with conformations of chains in corresponding regular model structures, all of which give RMS C_α model vs observed errors of less than 0.8 Å (Salemme and Weatherford, 1981a).

is clear that the observed structures fundamentally differ from the models because they incorporate heterogenous amino acid sequences. Thus it might be anticipated that non-uniformity of side-chain packing interactions could result in substantially larger local ϕ, ψ displacements from regularity than occur for reasons outlined above. Indeed, Chou and Scheraga (1982) demonstrated that extended polyvaline sheets were both substantially more twisted than polyalanine sheets, and were more conformationally irregular on unconstrained energy minimization. These results show that side chain interactions are of sufficient energetic magnitude to substantially alter the balance between polypeptide conformation and interchain hydrogen-bond optimization. Consequently, the frequently large apparent deviations in observed sheet chain conformations, in structures that are otherwise quite geometrically regular, appears to reflect local optimization of heterogeneous side chain packing (Fig. 32). As illustrated in Fig. 33, the major effect of such interactions is to produce a displacement at C_β which introduces a torsional force most readily resolved by rotations about the coparallel bonds in the polypeptide backbone. Such displacements result in only small displacements of the chains' C_α carbons, but are instead accommodated by rotations of the adjacent polypeptide planes (Ooi *et al.*, 1978). Rotation of the polypeptide planes, in turn, introduces associated deformations into the interchain hydrogen-bonds. The final configuration therefore again reflects a compromise between the local intra- and interchain packing interactions and the preservation of the interchain hydrogen-bonds.

An additional type of structural deformation which can produce substantial apparent discrepancies between observed and model β-sheet conformations is associated with peptide bond deviations from planarity. An initial investigation of the geometrical properties of twisted β-sheets illustrated that hydrogen-bonds in right-twisted sheets composed of straight-helical chains, were optimized if the peptide groups deviated from planarity

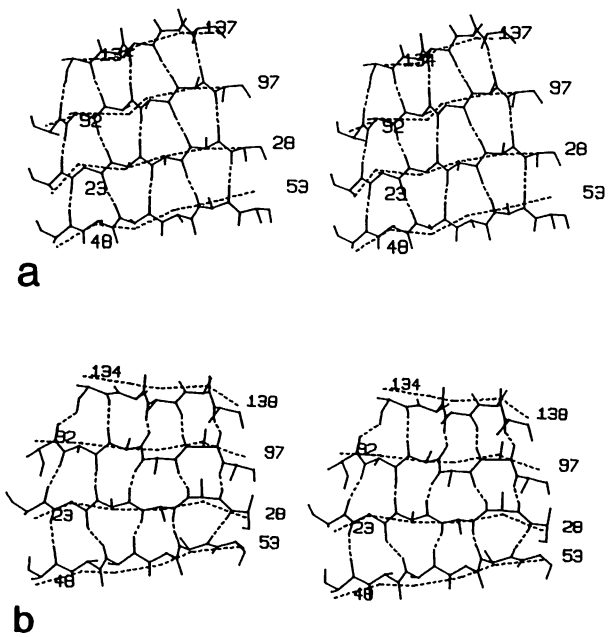

FIG. 32. (a) A least-squares fit of a conformationally regular model ($\phi = -114°$, $\psi = 124°$ average NHO bond length of 2.89 Å with a standard deviation of 0.15 Å) with the four most regular strands of the parallel β-sheet in lactate dehydrogenase. The average superposition error or corresponding model and observed α-carbon positions is 0.60 Å. (b) A least-squares fit of a generated model having regular polypeptide geometry, observed ϕ, ψ values, and least-squares optimized interchain hydorgen-bonds, fit to the observed structure. This model has more highly distorted interchain hydrogen-bonds (average length 3.08 Å with a standard deviation of 0.48 Å) and C_β packing interactions than the regular model. The average generated model vs observed structure α-carbon superposition error is 0.91 Å. Although this fit may be improved by fitting individual generated chains to each of the observed chains, the hydrogen-bonds of the resulting model structure become correspondingly worse than those of the hydrogen-bond optimized structure.

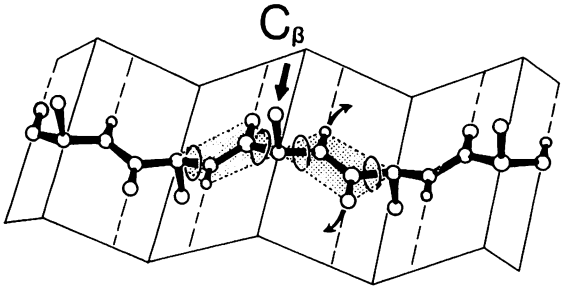

FIG. 33. Heterogeneous side-chain packing effects in β-sheets induce displacements at C_β which are accommodated by the rotation of adjacent peptide planes. This in turn results in apparently irregular local chain conformations and increased deformations in the interchain hydrogen-bonds. Note that the C_α carbons are at nodes for such displacements, so that regular structures accurately approximate the geometry of observed structures despite apparent local conformational variations (Figs 31 and 32).

(Weatherford and Salemme, 1979). Most interesting was the expectation that twisting the peptide plane could introduce sp^3 tetrahedral character into the amide nitrogen, so producing a second chiral center in the polypeptide backbone (Ramachandran and Kolaskar, 1973; Ramachandran *et al.*, 1973; Renugopalakrishnan and Rein, 1976) (Fig. 34). Residues with their peptide planes twisted in opposite directions would therefore be diasteriomers, and so differ energetically. In principal then, an energy difference between the opposite senses of peptide plane twist could contribute to the stabilization of twisted sheets. Chou and Scheraga (1982) investigated this point by energy minimizing a regular polyaline sheet structure where the peptide planes were allowed to twist. They in fact observed an

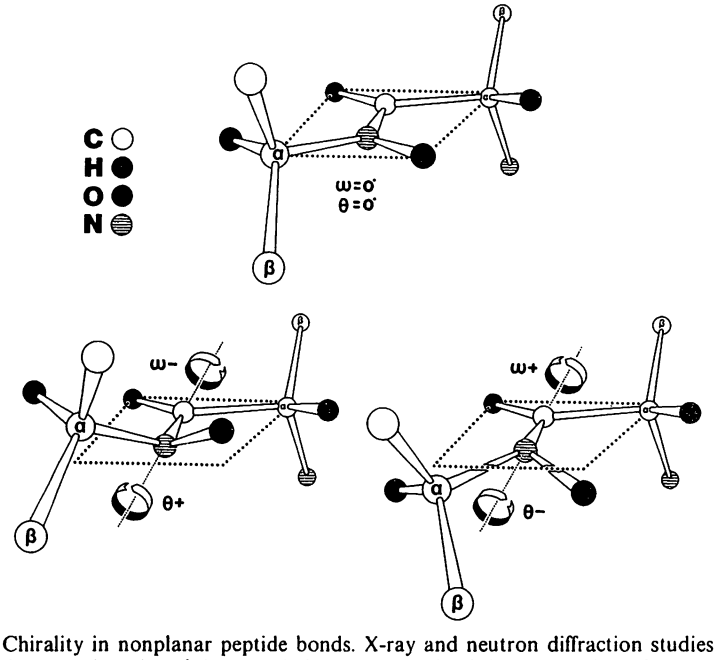

FIG. 34. Chirality in nonplanar peptide bonds. X-ray and neutron diffraction studies of peptides indicate that nonplanarity of the peptide bond is a result of the assumption of partial tetrahedral character by the peptide nitrogen atom. (a) Planar peptide with adjacent α-carbons showing the peptide plane with dashed lines. (b) Nonplanar peptide bond having local right-handed helical character. Two angles must be specified to describe such distortions: $\Delta\omega$, which is $\omega = -180°$ (ω being the angle between the $C\alpha_i$, C_i, N_{i+1} plane and the C_i, N_{i+1}, $C\alpha_{i+1}$ plane) and θ_N, which is the angle between the C_i, N_{i+1}, $C\alpha_{i+1}$ plane and the C_i, N_{i+1}, H_{i+1} plane. The figure shows a symmetrical distortion for which $\theta_N = -2\Delta\omega$. Peptide crystal structures show that values of θ_N vary from $-\Delta\omega$ to $-2\Delta\omega$ (Weatherford and Salemme, 1979). Peptide bond with $+\Delta\omega$, $-\theta_N$ tetrahedral character, such as preferentially observed in small peptides. Such nonplanar peptide bond distortions introduce local left-handed helical character into a polypeptide chain, and so are potentially favorable deformations in twisted β-sheets. The conformations shown in (b) and (c) are diastereomerically related.

overall tendency for the peptide planes to twist in the anticipated manner on energy minimization. As has been pointed out previously, this could be the consequence of minimizing the structure's overall energy at the expense of the amide bond planarity. However, this conclusion rests on assumptions concerning the nature of the potential function governing the amide bond twist. Most conformational energy parameterizations assume an amide twist potential with a minimum at the planar structure. In contrast, a variety of studies suggest that the amide twist potential which introduces tetrahedral character into the amide nitrogen has minima which correspond to ω values differing from 180° (Ramachandran and Kolaskar, 1973; Ramachandran *et al.*, 1973; Renugopalakrishnan and Rein, 1976). Thus, the question of whether peptide bond deformations either contribute favorably to, or occur at the expense of, the twisted structures' energy ultimately depend upon which description of the amide twist potential is applicable to β-sheets. The situation is further complicated as theoretical studies indicate that extended hydrogen-bond networks may be additionally stabilized through polarization effects (Sheridan and Allen, 1980). These charge delocalization effects are expected to be optimal in planar peptide arrays owing to improved π-orbital overlap between the sp^2 hybridized amide nitrogen and carbonyl carbon atoms. Relevant studies suggest that the extents of network polarization in arrays composed of five or six contiguously hydrogen-bonded peptides may significantly contribute to the stabilization of β-sheets which typically incorporate a comparable number of polypeptide chains (Sheridan and Allen, 1980; Sheridan *et al.*, 1982). Consequently, such polarization effects could act in opposition to the factors leading to the tetrahedral deformation of the peptide amide nitrogens typically observed in the crystal structures of small peptides (Weatherford and Salemme, 1979). Whatever the case, the application of neutron diffraction methods to proteins holds promise for experimentally investigating such effects, as this method allows direct determination of the hydrogen atom positions. At present, whether or not such deformations are observed in refined X-ray structures seems to reflect the nature of the constraints applied to insure a favorable ratio of observed data to refineable structural parameters.

VI. FUNCTIONAL CORRELATES OF β-SHEET ARCHITECTURE

The free energy change associated with folding a protein into its functional tertiary conformation typically lies in the range of a few tens of kilocalories per mole, or less (Privalov, 1979). As a consequence of this marginal stabilization, proteins in solution are dynamical structures owing to the constant interchange of thermal energy between them and the solvent environment (Cooper, 1976). In what follows, we consider how various features of β-sheet architecture relate to protein physicochemical properties in a dynamical environment.

1. *Structural Stabilization*

The preservation of protein functional integrity in solution depends ultimately on the structure's ability to resist or accommodate free energy fluctuations occurring as a consequence of collisions with solvent molecules. In principle, we can distinguish two extremes representing how a protein might accommodate dynamic loads associated with fluctuations in the structure's free energy. The first case would correspond to a structural arrangement with a deep and well-defined potential energy minimum (Fig. 35). Fluctuation-induced displacements in the structure are strongly resisted by the interactions defining the minimum, so that transient kinetic energy imparted during fluctuations is dissipated in rapid and localized collisional processes (McCammon *et al.*, 1977). We can describe structures with well-defined minima, which resist delocalized deformations, as being "rigid". Alternatively, we might imagine a structure with a less well-defined local minimum, which could undergo relatively large displacements as a consequence of free energy fluctuations. If the displacements in the structure correspond to excitation of cooperative vibrations involving large regions of the protein, the kinetic energy of transient fluctuations can be dissipated through viscous damping to the solvent environment. The notion of a cooperative structural deformation infers the existence of relatively well-defined pathways both for the structure

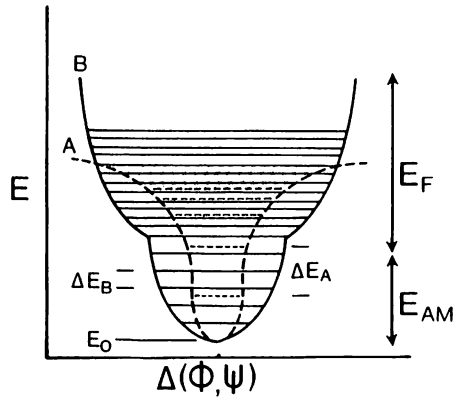

FIG. 35. A schematic plot of internal energy vs torsional displacements for coupled modes in protein secondary structures. Curve A (dashed) represents the potential surface for a "rigid" structure whose energy varies relatively rapidly as a function of coupled displacements in internal coordinates ϕ and ψ. For small displacements from the minimum potential energy (E_0), such as predominate at ambient temperatures over the range of energies E_{AM}, coupled motions may retain substantial harmonic character. However, for larger and less frequent energetic excursions occurring due to fluctuations in the range E_F, the structure encounters increasingly anharmonic restoring potentials. Such excursions may result in mode mixing, and local structural disruptions which provide mechanisms for dissipation of excess thermal energy from the structure. Curve B, in contrast, illustrates the potential surface behavior for coupled motions on a PTI like β-sheet. Owing to the conformational flexibility of this structure, the potential function governing excursions in its coupled modes retain predominant harmonic character for larger amplitude displacements in the internal torsional coordinates. Correspondingly, successive vibrational levels (ΔE_B) are more closely spaced than for a more rigid structure (ΔE_A), so that structure B is excited to a higher vibrational state at comparable temperatures, and has a higher librational entropy. Most interesting in the case of double helical antiparallel β-sheets, is the observation that larger energy fluctuations (in the range E_F), which may be sufficient to overcome stabilizing side-chain packing interactions (Fig. 23), do not disrupt the hydrogen-bonds responsible for coupling in the structure. This suggests that the structure's motions remain cooperative even for relatively large energetic fluctuations.

undergoing displacements from the minimum, and conversely, returning to the minimum after dissipating the excess energy of a fluctuation. The time-average stability of such a "flexible" structure therefore reflects its ability to accommodate transient fluctuations in relatively low frequency cooperative motions that return the structure to its potential energy minimum state (Salemme, 1982) (Fig. 35).

Real proteins exhibit dynamical behavior over a very wide time-scale (10^{-12} to 10^{-2} sec, or more), and so reflect a multitude of dynamic relaxation phenomena. Nevertheless, it is interesting to relate the structural properties of β-sheets to the simple model. This differentiates the structures according to whether they are (a) "rigid", and dissipate excess kinetic energy due to fluctuations in localized, high-frequency, collisional processes that are largely stochiastic in nature, or (b) "flexible", so that they dissipate kinetic energy through damping of cooperative lower-frequence vibrations in extended regions of the structure.

Several features of twisted parallel sheets suggest that they are structurally rigid. (1) Both geometrical and conformational energy studies show that the allowed chain conformations incorporated in twisted parallel sheets are more restricted than in antiparallel sheets (Salemme and Weatherford, 1981a). Moreover, conformational energy studies of twisted, parallel polyvaline sheets show that they have lower potential energies than corresponding antiparallel structures (Chou and Scheraga, 1982). Taken together, these results indicate that the minimum potential state of chains in parallel sheets is both deeper and more well-defined than for antiparallel sheets. (2) Twisted parallel sheets form extended surfaces with anticlastic curvature; both the saddle-shaped (hyberbolic paraboloid) and barrel (hyperboloid of revolution) parallel sheets form surfaces which are locally curved in opposite directions. Such surfaces find wide application in engineering practice both for their rigidity and ability to uniformly distribute applied loads (Otto, 1969). In architectural applications, the rigidity of these structures is further enhanced by their construction with prestressed composite materials (e.g. reinforced concrete). Twisted parallel β-sheets are similarly prestressed

because the potential energy minimum represents a situation where intra- and interchain non-bonded interactions act in opposition to the interchain hydrogen-bonding forces. (3) The strands of parallel β-structures are typically interconnected by regions of α-helix. The extended β-α-β arrays then correspond to a twisted surface composed of the sheet strands, on which is stacked a correspondingly twisted "sheet" of α-helices. It is interesting to consider the properties of these helix "sheets" in the present context, as these helix arrays also appear to be prestressed structures. Specifically, if we consider the helix sheets in isolation, we recognize that their organization again reflects a compensation between two opposing energetic factors. The first factor involves favorable packing interactions between the helices which tend to constrain interhelical angles in β-α-β arrays to about 20° (Richmond and Richards, 1978; Chothia *et al.*, 1980; Weber and Salemme, 1980). However, owing to the parallel arrangement of the α-helix macrodipoles in the structure, the dipolar interactions between the helices are energetically unfavorable (Hol *et al.*, 1981; Sheridan *et al.*, 1982), so stressing the helix sheet in the direction of increasing twist. Taking this view, it is additionally evident that the same geometrical constraints which result in the production of saddle-shaped vs barrel β-sheets (Fig. 5), are also operative in the production of the corresponding arrangements in sheets of α-helices. Moreover, the intimate packing attained between the β-sheet and the α-helix "sheet" in β-α-β structures, reflects that both the β-sheet strands and α-helices have potential energy minima which corresponds to interchain *and* interhelical twist angles of $\sim$20°. Thus, β-α-β domains are structures composed of layered stressed sheets of both α-helices and extended polypeptide chains, which are individually subject to geometrical constraints that insure intimate packing between them (Chothia *et al.*, 1980).

Antiparallel β-structures present a much more complicated picture owing to the observed diversity of their structural forms. For example, ongoing studies of multiple-strand antiparallel sheets suggest that similar principals of uniform stress distribution are determinative factors in sheet structural organization (Fig. 16), despite the fact that antiparallel sheets are by all criteria, intrinsically more flexible than parallel sheets. However, one antiparallel structural motif recurs whose properties fundamentally differ from those previously described. This is the double-strand antiparallel sheet, which typically occurs as a double-helical arrangement in known protein structures. In contrast to virtually all other sheets, the minimum potential energy configuration of the double-strand structure is achieved with essential preservation of energetically optimal interchain hydrogen-bonds (KenKnight and Salemme, in preparation). Thus, both intra- and interstrand interactions act collectively to stabilize the structure. In the preceding sense, this structure is unstressed in its minimum potential state, but is instead stabilized by interchain packing effects which arise owing to the structure's highly twisted conformation (Fig. 23). (Parallel double-strands cannot twist to the extent required for intimate side-chain packing. Consequently, they are not generally observed in protein structures except in isolated cases where less twisted sheets pack on α-helices to form small β-α-β domains.) Consider now the consequences of thermal fluctuations which will displace the structure from its potential energy minimum. Two cases can be distinguished. The first corresponds to the time-average dynamical behavior where the structure has the average kinetic energy of the thermal environment, $\sim kT$. Inspection of the potential energy surface for coiling (Fig. 29) illustrates that even the frequent small energy fluctuations characteristic of the average thermal environment can potentially cause substantial displacements in the cooperative motions of the structure. This implies that the structure's free energy of stabilization reflects not only potential, but kinetic (i.e. entropic) effects, as well (see below). In the second case, relatively infrequent but much larger fluctuations could occur, so driving the structure substantially farther from the potential minimum (Fig. 35). Such large fluctuations are presumably responsible for the transient accessibility and scission of internal hydrogen-bonds in proteins that render buried amide group protons exchangeable with solvent protons (Englander *et al.*, 1972). However, the smooth and continuous nature of the potential energy surface associated with sheet coiling (Fig. 29) suggests that even these large fluctuations can be accommodated by cooperative motions in the structure (Salemme, 1982). The time average stability of the structure therefore derives in part from its ability to accommodate large amplitude fluctuations in

motions that cooperatively return the structure to its potential minimum. Double-strand antiparallel β-sheets, and other antiparallel sheets to the extent that their local conformational minimum are governed by "soft" potential functions, consequently appear stable owing to their flexibility. They are structures that may accommodate transient loads by deforming elastically.

2. *β-Sheet Folding*

Essential to the rapidity of protein folding is the transient formation of a succession of intermediates, each of lower free energy and more completely resembling the final folded state. Aspects of both the temporal organization and cooperativity associated with folding are suggested by the foregoing description of β-sheet architecture. For example, it is presumably some statistical preference, related to the tendency for extended polypeptide chains to locally form left-helical conformations, which favors the right-handed coiling of polypeptide chains during initial stages of protein folding (but, see below). This could favor the assembly of β-α-β domains with "right-handed crossover" connections, as is almost invariably observed in known protein structures (Richardson, 1976, 1977, 1981; Sternberg and Thornton, 1976, 1977) (Fig. 36). Once an initial chain contact is made, one might readily

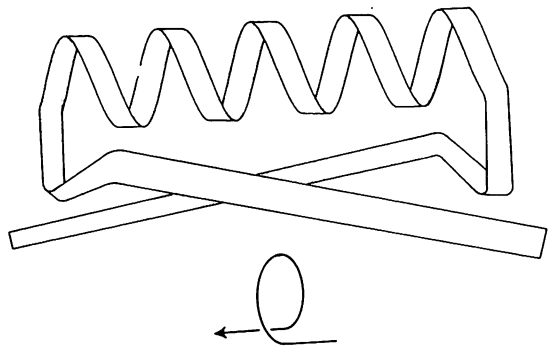

FIG. 36. Schematic of a local β-α-β domain typically seen in extended parallel sheets (Fig. 5). β-α-β domains have sheet strands interconnected by α-helices arranged with an overall right-handed supercoil sense.

imagine the successive formation of hydrogen-bonds to propogate a double strand sheet, and further chain coiling to extend the number of sheet chains. Whatever the nature of the structures' excursions during the process, it is clear that as more sheet hydrogen-bonds are formed, the sheets final conformation becomes progressively more well defined. Consequently, the constraints on chain conformation accompanying successive steps in interchain hydrogen bond formation determine how the structure can deform as a whole. The extended interactions in the sheet can therefore define both a cooperative folding pathway for the structure and the geometry of its final state (Salemme, 1982). The determinative step in β-α-β structural organization then becomes the initial formation of the interstrand hydrogen-bonds. According to whether the strands initially associate in aligned or staggered plan, the sheet will cooperatively fold to form either a saddle-surface or a barrel (Fig. 5).

Antiparallel sheets present a more complicated picture owing both to diversity in their hydrogen-bonding arrangements and final geometries relative to parallel sheets. However, many antiparallel sheets are folded in ways that suggest the involvement of hairpin-like double-strand structures as folding intermediates (Richardson, 1981). It is of consequent interest to consider how the properties of this sheet may relate both the stabilization of folding intermediates and the chiral folding of the final structure. Consider first the process of folding a double strand sheet into a double-helical coiled conformation. Figures 21 and 29 illustrate that there potentially exist a multitude of highly cooperative and similarly low-energy pathways for folding the structure from a variety of flat sheet conformations. While this would obviously provide a facile path for domain folding, it is useful to ask why this

situation might occur, rather than some arbitrarily large number of alternatives. Basically this is a result of the coupled nature of the hydrogen-bonded sheet. As illustrated by analogy in Fig. 37, a random polypeptide chain can be viewed as an ensemble of oscillators which behave essentially independently. However, formation of an extended β-sheet couples these oscillators so that they are no longer independent, and there emerges a new set of vibrational modes characteristic of the structure as a whole. The modes of lowest energy (and frequency) are those which correspond to collective motions in the structure (i.e. have high effective mass) that encounter weak restoring forces. Peticolas (1979) has pointed out that such soft collective modes in proteins are likely to be highly vibrationally excited at ambient temperature. Thus, a sheet undergoing cooperative oscillations achieves some transient free energy stabilization owing to the structure's librational entropy. The net effect is to drive the cooperative modes of the structure to large amplitude excursions, which indeed, correspond to highly cooperative folding trajectories for the double-helical domain as a whole. As outlined above in the context of structural stability, these entropic stabilization effects may persist even after the structure is folded, and so contribute to the stabilization of the folded domain structure (Sturtevant, 1977).

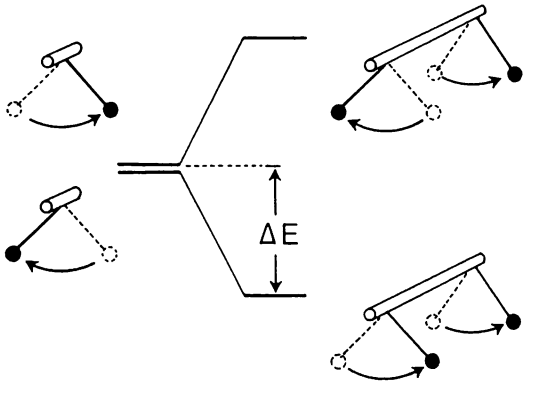

FIG. 37. A simple example of the effects of coupling oscillators. When initially independent oscillators are coupled together, there emerges a new set of vibrational modes characteristic of the structure as a whole. As a result, kinetic energy is partitioned differently in the coupled structure.

Many multiple-strand antiparallel sheets observed in proteins are organized in ways which suggest their folding from double-strand intermediates (Richardson, 1982). Perhaps the simplest examples are the "jelly-roll" β-sheets. This is an arrangement where a double strand hairpin sheet is coiled around a cylindrical surface to produce an extended hydrogen-bonded sheet (Fig. 38). The sense of the coiling is always observed to be "right-handed", i.e. the hairpin follows a right-handed helical path on the cylinder surface. The invariance of this chiral property in these structures (as well as the "right-handed" β-α-β crossover connections described above (Fig. 36)) is of some interest because there exists no *a priori* relationship between the sense of the local polypeptide chain helix and its supercoiling sense (Nishikawa and Scheraga, 1976). However, a more careful analysis of double-strand coiling suggests how this situation might arise. Consider first the cooperative coiling of a simple double-helical structure from a flat sheet. The salient point is that the two surfaces of a *double-stranded antiparallel* sheet are different, one surface being populated by residues situated in "small" hydrogen-bonded rings, and the other by residues in "large" rings (Fig. 2). In principle, two alternative double helical arrangements could be imagined, both of which are "right-handed", but which differ according to the situation of the small and large ring substituents relative to the structures coil axis (Fig. 39). The fact that only one of these alternatives is actually observed, with the small ring residues on the coil interior, is a consequence of the structural properties of the double-strand sheet. Specifically, coiling the sheet involves the cooperative superposition of both components of sheet twist and bend (Fig. 28). Both of these deformation components are asymmetric in the production of a

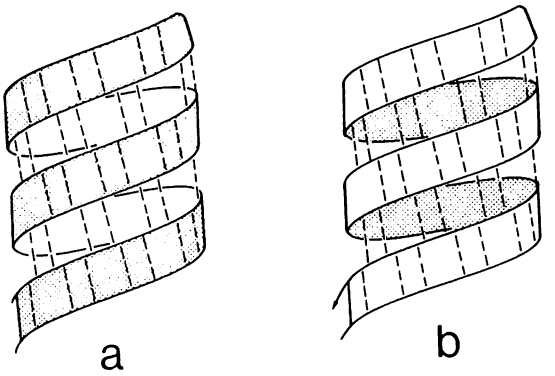

FIG. 38. Right-supercoiled β-sheets form "jelly-roll" structures which suggest their folding from double-strand hairpin intermediates. However, a double-strand sheet has surfaces which differ (Fig. 2), so that two alternative coiled arrangements ((a) and (b)) can potentially be envisioned. Studies of the potential energy surfaces governing cooperative coiling of antiparallel sheets suggests facile folding pathways only for arrangement (b). This folds from a double-strand intermediate with "small-ring" residues situated on sheets concave surface (Fig. 39).

double helical coil which preserves the interchain hydrogen-bonds; the chains locally twists in a left-handed sense, and the sheet bends as a whole, with the small ring residues on the concave surface (Fig. 39) (in fact, "left-handed" coils exhibit the same bend asymmetry). The chiral coiling of the structure therefore fundamentally reflects a coupling between asymmetric sheet twist and an asymmetric bend that results from geometrical constraints imposed by the interchain hydrogen-bonds.

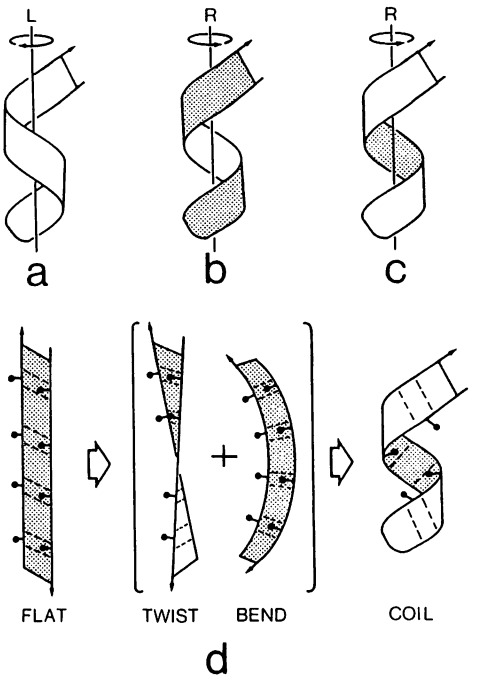

FIG. 39. Chiral coiling in antiparallel hairpin sheets. Part (a) illustrates a left-hand coiled sheet (unobserved in protein structures), while (b) and (c) illustrate alternative right-coiled structures where the small ring substituent surface (Fig. 2) (shaded) is oriented alternatively toward or away from the supercoil axis. In isolated β-coils (as in pancreatic trypsin inhibitor, Fig. 23) the small ring surface is always on the structure interior (c). Part (d) illustrates that this is a consequence of a coupling between sheet twist and bend, both of which are asymmetric (Fig. 26). These effects act in concert to produce the observed chiral supercoil geometry, both in this and more extended structures (Fig. 38). These results suggest that the observed chiral supercoiled arrangements must result from cooperative folding of a double-strand intermediate, since the asymmetry in bend required to produce the structures is a unique property of the double-strand sheet. The local chain twist, in contrast, is a property of all extended polypeptides composed of L-amino acids.

The emergence of chiral folding patterns in multiple-strand antiparallel β-sheets (e.g. Fig. 38) therefore appears as a consequence of the coupling between sheet twist and bend that is necessarily associated with the transient formation of double-strand intermediates in folding. This model predicts that observed "jelly-roll" structures should conform to the sheet orientation pattern shown in Fig. 33(b), where the structure is folded by supercoiling a double-strand intermediate which bends with its "small-ring" surface oriented towards the structure's interior (Fig. 39). Otherwise, in the final folded state where all the hydrogen bonds are formed, the structures diagrammed in Fig. 33(a) and 33(b) would be expected to be energetically equivalent.

3. *Functional Implications*

A recurrent theme in this discussion has been the distributed nature of forces determining β-sheet structural geometry, folding pathways, and response to fluctuations in free energy. However, the spatial and temporal cooperativity implicit in these structures suggests correlations with protein function that go beyond the structural and physicochemical questions addressed previously.

Allostery represents one aspect of protein function where ligand-protein interactions at sites remote from the catalytic site affect protein function. At least two different sorts of effects might be envisioned which reflect the cooperative properties of β-sheets. Effector ligand binding to the protein could alter the way in which the sheet strands were coupled together, so causing the sheet to cooperatively deform to a new minimum energy configuration. This could result in the propagation of a mechanical displacement through the sheet, that could in turn alter the spatial arrangements of catalytic residues in the protein's active site. Owing to the cooperative nature of β-sheet twisting, a very small alteration in chain conformation at one edge of the sheet could be amplified into a relatively large spatial displacement at the other. Conformational energy studies suggest that such alterations in sheet twist are energetically reasonable, because while the energies of homopolymer sheets vary slowly with the extent of twist, changes in residue type (or anything else that alters interchain interactions) can result in significantly different twisted conformations (Chou and Scheraga, 1982).

Sturtevant (1977) has suggested that one source of free energy differences on ligand binding results from alterations in the protein's librational entropy. A second ligand binding effect might therefore involve alteration of the potential function governing thermally excited cooperative oscillations in the β-sheets (Salemme, 1977; Watt and Sturtevant, 1969). Such effects would appear most relevant to structures composed of antiparallel sheets, as they are relatively more flexible than the usually stressed parallel sheets. Few allosteric proteins incorporating β-sheets are currently known in sufficient structural detail to verify these proposals. However, it is possible that the hinge bending motions occurring in hexokinase (MacDonald *et al.*, 1979) and arabinose binding protein (Mao *et al.*, 1982) could reflect cooperative alterations in the twist of the sheets interconnecting structural domains in these molecules. On the other hand, inelastic neutron scattering studies on hexokinase, in both liganded and unliganded forms, suggest alterations in the molecule's vibrational properties on glucose binding (Jacrot *et al.*, 1982). Thus it may be that both static and dynamical alterations in structural architecture result as a consequence of ligand binding. In the current context, "static" variations in β-sheet twist might be expected to simultaneously modify sheet vibrational properties, since altering the sheet minimum energy geometry is similarly likely to alter the potential surface governing displacements in the vicinity of the minimum.

Rate-limiting steps in enzyme catalysis typically involve processes where activation energy barriers must be overcome in order to convert a substrate into an intermediate or product. The reaction rate is thus a measure of the frequency with which *particular* fluctuations occur of sufficient free energy to surmount the activation energy barrier. A major motivation for investigating protein dynamics (McCammon *et al.*, 1977) stems from the possibility that structural fluctuations *characteristic of a particular enzyme* assist in the catalytic process (Careri *et al.*, 1979). More specifically, it is possible that thermally-driven cooperative

motions can localize dynamic deformations at an enzyme's active site. These dynamic forces could transiently deform a substrate to facilitate intermediate formation, or alter hydrogen-bonding arrangements among active site residues to facilitate general acid or base catalysis. Although little is currently known about such processes, twisted β-sheets are structures which can apparently localize structural deformation forces. Consider, for example, an extended protein β-sheet which undergoes oscillations in twist. From the foregoing description of the properties of these structures, it is apparent that structural deformations tend to be greatest at the sheet boundaries where they are unconstrained by hydrogen-bonds. Similarly, sheet twist oscillations will transiently increase deformations at sheet edges, so that the net effect of the cooperative sheet twisting is to concentrate deformation forces at the sheet boundary. If, as for many proteases, substrate binding essentially extends a preexisting sheet in the protein (Kraut, 1977), it is possible that twist oscillations in the resulting extended sheet could transiently deform the substrate in a manner facilitating catalysis.

Evidence for the localization of deformation forces in protein β-sheets comes from neutron diffraction (Wlodawer and Sjolin, 1982, Kossiakoff, 1982) and NMR (Wagner and Wuthrich, 1979; Wuthrich and Wagner, 1979) studies which examine the structural situation of non-exchangeable amide protons in proteins. The exchange of ostensibly solvent inaccessible hydrogen-bonded protons from the protein interior is the result of energetic fluctuations in the protein structure (Englander *et al.*, 1979). Amide proton exchange is consequently a process which reflects both the transient accessibility of buried groups and the localization of dynamic stresses which sever internal hydrogen-bonds, as required for their facile exchange with solvent protons. In the structures examined thus far, amide protons found to be particularly resistant to exchange have been predominantly localized in regular extended regions of antiparallel sheet. This result is basically consistent with the idea that antiparallel sheets are flexible, and can accommodate transient fluctuations as cooperative motions that incur little stress on the interchain hydrogen-bonds (Salemme, 1982). On the other hand, exchange from the less-regular regions and/or peripheries of these sheets is observed to be

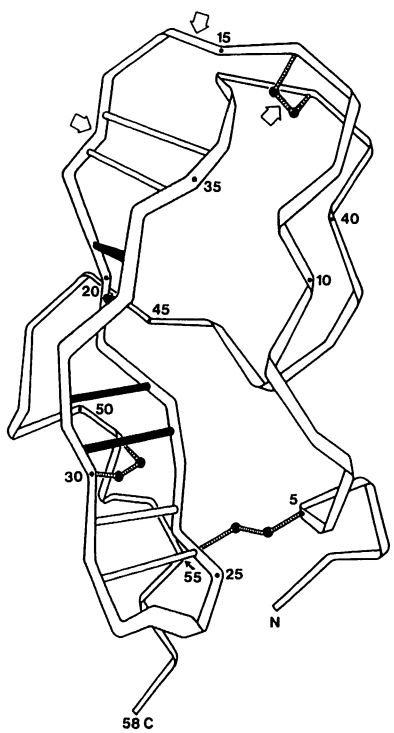

FIG. 40. A ribbon drawing of pancreatic trypsin inhibitor emphasizing the double helical, antiparallel β-sheet (shaded) incorporating residues 17-36. Of the groups forming interchain hydrogen-bonds in the sheet (illustrated as rungs interconnecting the polypeptide chain), four in the center of the sheet (solid rungs) incorporate peptide amide groups which are unusually resistant to exchange with solvent protons, whereas those at the sheet ends exchange much more rapidly.

relatively rapid. Figure 40 schematically illustrates pancreatic trypsin inhibitor (Deisenhofer and Steigemann, 1975), a small protein incorporating a highly symmetric double-strand antiparallel coil. The hydrogen-bonds in the center of this sheet are unusually resistant to exchange, a feature which has been suggested to relate to the extraordinary cooperative flexibility of the structure (Fig. 24). This flexibility depends fundamentally on the structure's preservation of symmetry (i.e. structural equivalence of the hydrogen-bonds) when it undergoes fluctuation-induced oscillations. However, structural interactions at the sheet ends, where it is sharply folded over or connected by a hairpin bend (Fig. 40), constrain the structure from undergoing the required symmetric motion in these regions of the sheet. As a result, dynamic stresses are localized at the sheet ends, so that the hydrogen-bonds there are stressed and broken more frequently than those in the sheet center. The localization of stresses owing to coupling with a cooperative sheet motion could be relevant to some aspects of enzyme catalysis in the following manner. While the foregoing has illustrated how stress localizations can sever interchain hydrogen-bonds, similar processes could occur which involve transient deformation in side-chain hydrogen-bond networks. This could, in turn, transiently facilitate proton transfers and/or general acid-base catalysis by residues at the protein active site. The important point is that the occurrence of such localized, and potentially catalytically useful, deformations must ultimately depend upon the long-range structural architecture of the protein. This suggests that an enzyme structure is not simply a rigid framework providing specific geometrical interactions facilitating substrate catalysis. Instead, enzymes are organized molecules which appear to accommodate the fluctuations incurred in a thermally active environment as cooperative motions that may transiently correlate the succession of high activation energy steps typically encountered in enzymatic catalysis (Salemme, 1982).

VII. CONCLUSIONS

X-ray crystallography has revealed proteins to be organized structures of marvelous complexity. Although we are far from understanding protein structure, in the sense that would allow an enzyme to be designed from first principles, the recurrence of particular structural features has provided a framework from which a fundamental understanding of their properties is beginning to emerge. The objective of the current treatment has been to illustrate that proteins are not simply compact aggregates of connected amino acids. Instead, they reflect highly refined solutions to the problem of maintaining structural stability in a dynamically active environment. While the role of protein dynamics in protein function remains to be unequivocally demonstrated, the idea that an organized structure can convert stochastic energy fluctuations in the environment into catalytically useful cooperative motions remains an intriguing prospect.

ACKNOWLEDGEMENTS

Thanks are due to Charles KenKnight who carried out the conformational energy computations on coiled antiparallel β-sheets. Work in this laboratory is supported by grants from the National Institutes of Health (GM 21534 and GM 30393) and the University of Arizona Computer Center.

REFERENCES

BANNER, D. W., BLOOMER, A. C., PETSKO, G. A., PHILLIPS, D. C., POGSON, C. I., WILSON, I. A., CORRAN, P. H., FURTH, A. J., MILMAN, J. D., OFFORD, R. E., PRIDDLE, J. D. and WALEY, S. G. (1975) *Nature (London)* **255**, 609–614.

BOYS, C. V. (1959) In *Soap Bubbles*, pp. 55–58, Dover, New York.

CARERI, G., FASELLA, P. and GRATTON, E. (1979) *A. Rev. Biophys. Bioeng.* **8**, 69–97.

CHOTHIA, C. (1973) *J. molec. Biol.* **75**, 295–302.

CHOTHIA, C., LEVITT, M. and RICHARDSON, D. (1980). *J. molec. Biol.* **145**, 215–250.

CHOTHIA, C. and JANIN, J. (1982) *Biochemistry* **21**, 3955–3965.

CHOTHIA, C. (1983) *J. molec. Biol.* **163**, 107–117.

CHOU, K. C. and SHERAGA, H. A. (1982) *Proc. natn. Acad. Sci. U.S.A.* **79**, 7047–7051.

CHOU, K. C., POTTLE, M., NEMETHY, G., UEDA, Y. and SCHERAGA, H. A. (1982) *J. molec. Biol.* **162**, 89–112.

COHEN, F. E., STERNBERG, M. J. E. and TAYLOR, W. R. (1981) *J. molec. Biol.* **148**, 253–272.

COHEN, F. E., STERNBERG, M. J. E. and TAYLOR, W. R. (1982) *J. molec. Biol.* **156,** 821–862.
COOPER, A. (1976) *Proc. natn. Acad. Sci. U.S.A.* **73,** 2740–2741.
DEISENHOFER, J. and STEIGEMANN, W. (1975) *Acta. Crystallogr.* **B-31,** 238–251.
ENGLANDER, S. W., DOWNER, N. W. and TEITLEBAUM, H. (1972) *A. Rev. Biochem.* **41,** 903–924.
FELDMANN, R. J. (1976) *Atlas of Macromolecular Structures on Microfiche*, Tractor-Jitco, Rockville.
GELLERT, W., KUSTNER, H., HELLWICH, M. and KASTNER, H. (1977) In *VNR Concise Encyclopedia of Mathematics*, pp. 544–547, Van Nostrand, New York.
HAGLER, A. T., LIFSON, S. and HUTLER, E. (1974) In *Peptides, Polypeptides and Proteins* (eds. E. R. BLOUT, F. A. BOVEY, M. GOODMAN and N. LOTAN), pp. 35–48, Wiley Interscience, New York.
HOL, W. G. J., HALIE, L. M. and SANDER, C. (1981) *Nature (London)* **294,** 532–536.
JACROT, B., CUSACK, S., DIANOUX, A. J. and ENGLEMAN, D. M. (1972) *Nature (London)* **300,** 84–86.
KOSSIAKOFF, A. A. (1982) *Nature* **296,** 713–721.
KRAUT, J. (1977) *A. Rev. Biochem.* **46,** 331–359.
LEVITT, M. and CHOTHIA, C. (1976) *Nature (London)* **261,** 552–558.
LIFSON, S. and SANDER, C. (1979) *Nature (London)* **282,** 109–111.
MACDONALD, R. C., STEITZ, T. A. and ENGLEMAN, D. M. (1979) *Biochemistry* **18,** 338–342.
MAO, B., PEAR, M. R., MCCAMMON, J. A. and QUICHO, F. A. (1982) *J. biol. Chem.* **257,** 1131–1133.
MATTHEWS, B. W., FENNA, R. E., BOLOGNESI, M. C., SCHMID, M. F. and OLSON, J. M. (1979) *J. molec. Biol.* **131,** 259–285.
MCCAMMON, J. A., GELIN, B. R. and KARPLUS, M. (1977) *Nature* **277,** 585–590.
MOMANY, F. A., MCGUIRE, R. F., BURGESS, A. W. and SCHERAGA, H. A. (1975) *J. phys. Chem.* **79,** 2361–2381.
NISHIKAWA, K. and SCHERAGA, H. (1976) *Macromolecules* **9,** 395–401.
OOI, T., NISHIAWA, K., OOBATAKE, M. and SCHERAGA, H. A. (1978) *Biochim. biophys. Acta* **536,** 390–406.
OTTO, F. (1969) *Tensile Structures*, MIT Press, Cambridge, Mass.
PAULING, L. and COREY, R. B. (1951) *Proc. natn. Acad. Sci. U.S.A.* **37,** 729–740.
PETICOLAS, W. L. (1979) *Meth. Enzymol.* **61,** 425–456, Part H.
PRIVALOV, P. L. (1979) *Adv. Prot. Chem.* **33,** 167–241.
RAGHAVENDRA, K. and SASISEKHARAN, V. (1979) *V. Int. J. Peptide Protein Res.* **14,** 326–338.
RAMACHANDRAN, G. (1974) In *Peptides, Polypeptides and Proteins* (eds. E. BLOUT, F. BOVEY, M. GOODMAN and N. LOTAN), pp. 14–34, Wiley Interscience, New York.
RAMACHANDRAN, G. N. and KOLASKAR, A. S. (1973) *Biochim. biophys. Acta* **303,** 385–388.
RAMACHANDRAN, G. N., LAKSHMINARAYAN, A. V. and KOLASKAR, A. S. (1973) *Biochim. biophys. Acta* **303,** 8–13.
RENUGOPALAKRISHNAN, V. and REIN, R. (1976) *Biochim. biophys. Acta* **434,** 164–168.
RICHARDSON, J. S. (1981) *Adv. Prot. Chem.* **34,** 167–339.
RICHARDSON, J. S., GETZOFF, E. D. and RICHARDSON, D. C. (1978) *Proc. natn. Acad. Sci. U.S.A.* **75,** 2574–2578.
RICHARDSON, J. S. (1977) *Nature (London)* **268,** 495–500.
RICHARDSON, J. S. (1976) *Proc. natn. Acad. Sci. U.S.A.* **73,** 2619–2623.
RICHMOND, T. J. and RICHARDS, F. M. (1978) *J. molec. Biol.* **119,** 537–555.
SALEMME, F. R. (1977) *A. Rev. Biochem.* **46,** 299–329.
SALEMME, F. R. (1981) *J. molec. Biol.* **146,** 143–156.
SALEMME, F. R. (1982) *Nature (London)* **299,** 754–756.
SALEMME, F. R. and WEATHERFORD, D. W. (1981a) *J. molec. Biol.* **146,** 101–117.
SALEMME, F. R. and WEATHERFORD, D. W. (1981b) *J. molec. Biol.* **146,** 119–141.
SHERIDAN, R. P., LEVY, R. M. and SALEMME, F. R. (1982) *Proc. natn. Acad Sci. U.S.A.* **79,** 4545–4549.
SHERIDAN, R. P. and ALLEN, L. C. (1980) *Biophys. Chem.* **II,** 133–136.
STERNBERG, M. J. E. and THORNTON, J. M. (1977) *J. molec. Biol.* **110,** 269–283.
STERNBERG, M. J. E. and THORNTON, J. M. (1976) *J. molec. Biol.* **105,** 367–382.
STURTEVANT, J. M. (1977) *Proc. natn. Acad. Sci. U.S.A.* **74,** 2236–2240.
WAGNER, G. and WUTHRICH, K. (1979) *J. molec. Biol.* **134,** 75–94.
WATT, G. D. and STURTEVANT, J. M. (1969) *Biochemistry* **8,** 4567–4571.
WEBER, P. C. and SALEMME, F. R. (1980) *Nature (London)* **287,** 82–84.
WEATHERFORD, D. W. and SALEMME, F. R. (1979) *Proc. natn. Acad. Sci. U.S.A.* **76,** 19–23.
WLODAWER, A. and SJOLIN, L. (1982) *Proc. natn. Acad. Sci. U.S.A.* **79,** 1418–1422.
WUTHRICH, K. and WAGNER, G. (1979) *J. molec. Biol.* **130,** 1–18.